*remote sensing*

MDPI

*Review*

# Evolution of Forest Tree DBH Measurement Technologies: From Contact-Based Traditional Approaches to Remote Sensing Non-Contact Methods

**Guohao Zhang , Zhanhui Li and Weixing Xue ***

College of Resources and Environment, South China Agricultural University, Guangzhou 510640, China; 20243180012@stu.scau.edu.cn (G.Z.); 20253180004@stu.scau.edu.cn (Z.L.)
* Correspondence: weixingxue@scau.edu.cn

## Highlights

### What are the main findings?

- This study systematically sorts out the research progress of forest tree diameter at breast height (DBH) measurement technologies from traditional contact-based methods to remote sensing non-contact methods, and elaborates on the core technical characteristics of mainstream photogrammetry and laser scanning platforms; it also establishes a multi-dimensional evaluation system for DBH measurement technologies, and conducts a comparative analysis of the performance trade-offs of typical methods.
- This study analyzes the multi-source fusion technology for DBH estimation from the three levels of data, feature and decision, identifies the core challenges in its practical forestry applications, and proposes targeted and feasible solutions accordingly.

### What are the implications of the main findings?

- The technical sorting results and multi-dimensional evaluation system of this study provide a scientific basis for the selection of DBH measurement technologies in forest inventory, and clearly define the performance boundaries and scenario adaptability of various mainstream methods.
- The analysis results of multi-source fusion technology and the corresponding solutions proposed in this study identify the core technical path to break through the observational limitations of single sensors, and provide operable guidance for improving the robustness of DBH estimation in complex forest stands.

## Abstract

Diameter at Breast Height (DBH) is a key parameter in forest measurement. However, existing research has mostly focused on improving the accuracy of individual technologies, lacking a systematic synthesis of the evolutionary logic of measurement techniques and a standardized selection framework for forestry applications. To this end, this paper constructs a multi-level classification framework based on measurement platforms and technical principles, establishes for the first time a five-dimensional comprehensive evaluation system (covering accuracy, efficiency, cost, environmental adaptability, and automation) along with a hierarchical technology decision tree, and systematically analyzes the application logic of multi-source fusion technologies across three levels: ground-based, near-ground mobile, and aerial. The review indicates that traditional contact-based measurement has limited efficiency; modern remote sensing technologies (photogrammetry and LiDAR) offer significant advantages in automation and accuracy, but still face challenges such as high equipment costs, complex data processing, and poor environmental

Check for updates

Academic Editors: Zengyuan Li, Erxue Chen and Lin Cao

Received: 11 February 2026
Revised: 13 April 2026
Accepted: 15 April 2026
Published: 18 April 2026

**Copyright:** © 2026 by the authors. Licensee MDPI, Basel, Switzerland. This article is an open access article distributed under the terms and conditions of the Creative Commons Attribution (CC BY) license.

adaptability. Multi-source fusion and machine learning are key methods to overcome the limitations of single sensors and improve the robustness of DBH estimation. Finally, it is anticipated that with decreasing sensor costs and the advancement of intelligent algorithms, DBH measurement will continue to evolve toward automation, intelligence, and engineering practicality, providing technical support for large-scale, long-term, and repeatable forest monitoring.

**Keywords:** diameter at breast height; diameter measurement; forest inventory; laser scanning; photogrammetry

## 1. Introduction

Diameter at breast height (DBH) is the most fundamental core factor in forest resource inventories. Measurement errors in DBH are progressively amplified through models, directly affecting the accuracy of carbon stock estimates at stand and even regional scales [1]. The iterative upgrading of DBH measurement technology is essentially an adaptation process driven by three pairs of contradictions: accuracy versus efficiency, cost versus coverage, and manual operation versus automation. Traditional DBH tape and calipers offer high accuracy but extremely low efficiency [2–6]; optical dendrometers achieve non-contact measurement but are limited to single-station operation; LiDAR, through active detection and integration with mobile platforms, achieves a high-level balance between accuracy and efficiency.

However, existing studies have mostly focused on improving the accuracy of individual technologies or validating them in specific scenarios, lacking a systematic review of the evolutionary logic of DBH measurement technologies and a standardized selection framework for practical forestry applications. Specifically, what are the performance boundaries and applicable conditions of different technologies—ranging from contact-based methods to photogrammetry, LiDAR, and even multi-source fusion—across the five dimensions of accuracy, efficiency, cost, environmental adaptability, and automation? Can multi-source fusion technologies overcome the dilemma of balancing accuracy, efficiency, and cost in complex forest stands? How can actionable technology selection rules be provided for different survey scales and site conditions?

To address the above issues, the core innovative contributions of this paper are (1) the construction of a five-dimensional comprehensive evaluation system covering accuracy, efficiency, cost, environmental adaptability, and automation; and (2) the proposal of a three-level technology decision tree oriented toward engineering practice, incorporating survey scale, site conditions, and accuracy requirements. On this basis, the paper systematically traces the complete evolutionary trajectory from traditional contact-based to modern non-contact measurement (see Figure 1), and critically analyzes the implementation pathways and key bottlenecks of multi-source fusion technologies at three levels: data-level, feature-level, and decision-level. The review indicates that traditional methods have limited efficiency; modern remote sensing technologies (photogrammetry and LiDAR) offer significant advantages in automation and accuracy, but still face challenges such as high costs, complex processing, and poor environmental adaptability; multi-source fusion and machine learning are key directions for overcoming the limitations of single sensors and improving robustness. The review indicates that traditional methods have limited efficiency; modern remote sensing technologies (photogrammetry and LiDAR) offer significant advantages in automation and accuracy, but still face challenges such as high costs, complex processing, and poor environmental adaptability; multi-source fusion and machine

learning are key directions for overcoming the limitations of single sensors and improving robustness. This paper aims to provide systematic and actionable technical references for forest resource inventory and sustainable management, and to promote the evolution of DBH measurement toward automation, intelligence, and engineering practicality.

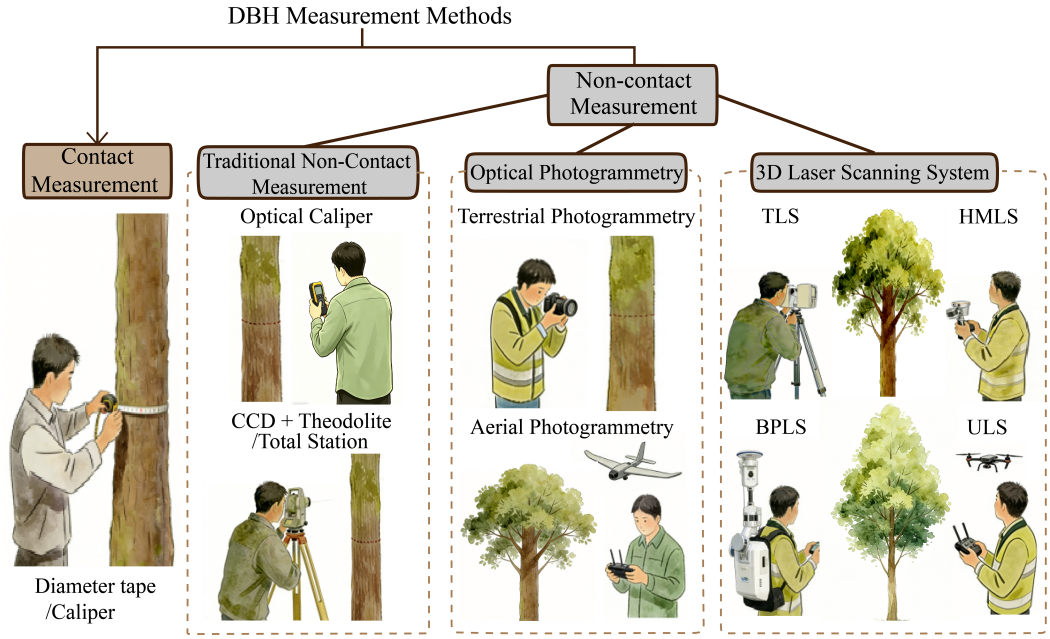



**Figure 1.** Classification framework and evolutionary path of DBH measurement technologies. Note: This framework takes measurement platform and technical principle as its two dimensions, dividing DBH measurement methods into three major stages—traditional contact, traditional non-contact, and modern remote sensing—which are further subdivided into nine technical pathways.

## 2. Traditional DBH Measurement Methods

Traditional DBH measurement methods are mainly divided into two categories: contact-based (e.g., DBH tape, caliper) and non-contact (e.g., optical dendrometer, total station, camera combination). The main thread of their improvement has been to prioritize efficiency and accessibility while meeting basic accuracy requirements.

### *2.1. DBH Tape and Caliper Measurement*

Contact-based measurement (e.g., DBH tape and caliper) is the industry-recognized accuracy benchmark. The DBH tape, which calculates diameter by measuring the circumference, offers extremely low cost, simple operation, and good repeatability, making it suitable for long-term monitoring in permanent sample plots. However, its error is shape-sensitive: when the stem cross-section is elliptical, twisted, or has burls, circumference measurement tends to overestimate the equivalent diameter [7]. The caliper avoids the conversion from circumference to diameter by directly measuring the diametrical distance, offering a more pronounced advantage in large-diameter tree measurement [8]. However, the error of the caliper is more susceptible to operator influence, such as the choice of cross-sectional position, clamping force, and fitting angle, all of which may introduce bias. More importantly, both methods are contact-based and require manual access to breast height, which is limited by accessibility, safety, and stand obstructions, resulting in extremely low efficiency in large-sample or complex terrain plots. This indicates that although contact-based measurement can serve as a benchmark for accuracy validation, its efficiency limitation of tree-by-tree operation makes it impractical for large-scale surveys.

### *2.2. Traditional Non-Contact Measurement*

Traditional non-contact measurement methods (e.g., optical dendrometers, total station, camera combinations) were introduced in the mid-to-late 20th century to overcome the spatial constraints of contact-based approaches. Optical dendrometers [9] (e.g., Criterion, Tele-Relaskop) achieve non-contact readings from several meters away using fixed fields of view and built-in scales. Total stations or theodolites combined with cameras can establish geometric models to obtain multiple parameters such as DBH and tree height [10–12]. These methods bring three substantial improvements: no need to contact the trunk, reduced inter-observer variability, and the ability to integrate multi-parameter acquisition. However, a comparison of various optical dendrometers by Parker et al. [13] showed that DBH error and stability vary significantly among instruments, and performance is highly dependent on the specific measurement geometry. Although total stations can obtain multi-section diameters without felling trees, their bulk, cost, and operational complexity make deployment difficult in high-canopy-closure or topographically complex areas. Subsequent domestically developed digital diameter measurement devices [14] (e.g., handheld digital tree measurement guns [15], micro total stations [16]) achieve a certain balance between accuracy and portability, but still require tree-by-tree aiming or close-range measurement. This essentially replaces manual reading with instrument reading, without fundamentally resolving the efficiency bottleneck of tree-by-tree operation.

Overall, the evolution of traditional DBH measurement—from contact-based to non-contact, from manual reading to instrument-based reading, and from single-parameter to multi-parameter integration—has essentially prioritized efficiency and accessibility within acceptable accuracy constraints. However, the introduction of instruments brings new issues such as cost and power supply, and the methods remain limited in complex stands and terrains. These challenges have laid the foundation for subsequent technological pathways, such as lighter, smarter modern photogrammetry and 3D laser scanning.

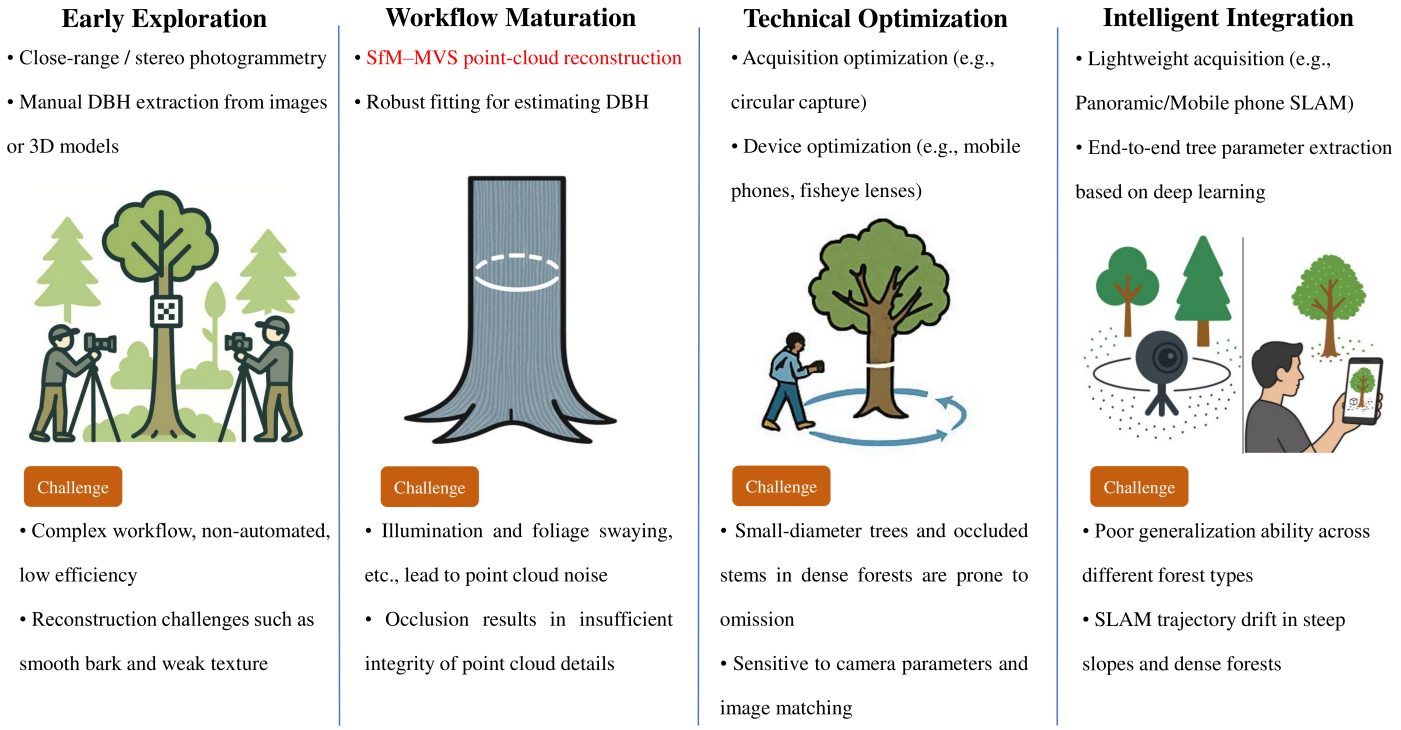
## 3. DBH Estimation Based on Optical Photogrammetry

Structure from Motion (SfM) and Multi-View Stereo (MVS) constitute an integrated computer vision workflow for 3D reconstruction from multiple 2D images [17–19]: the SfM algorithm jointly estimates the 3D structure of a scene and camera parameters from images taken from different viewpoints to generate a sparse point cloud; MVS conducts dense matching on images based on these camera parameters to produce a dense point cloud, thus facilitating the acquisition of a detailed 3D model. Unlike traditional stereo photogrammetry, this method does not require pre-known camera positions, orientations, camera calibration, or control points in the scene, thereby allowing 3D reconstruction to be performed with low-cost imaging devices in various application scenarios, including aerial and terrestrial ones. The increasingly mature SfM-MVS algorithm, combined with terrestrial and aerial photogrammetry, enables automated, non-contact, high-precision measurement of DBH. Their applications have gradually garnered widespread attention in the field of forest surveying and mapping.

### *3.1. Terrestrial Photogrammetry*

Early terrestrial photogrammetry mostly adopted close-range/stereo photogrammetry workflows [20,21]. Although it had low equipment thresholds and was portable and easy to operate, it suffered from low automation and standardization levels, making it unsuitable for large-scale forestry surveys. With the deep integration of SfM-MVS technology and terrestrial photogrammetry, three-dimensional reconstruction of tree trunks and automatic DBH extraction can be achieved, significantly improving the automation level and operational efficiency of non-contact diameter measurement. Existing studies have conducted

systematic analyses in multiple directions [22–25], and extensive research has been carried out on lightweight device adaptation [26–29], edge-side real-time calculation [30–33], and measurement accuracy breakthroughs [34,35] targeting the existing pain points of this technology (Figure 2).




*Note: The content highlighted in red contributes to a substantial improvement in measurement accuracy. Challenges at each stage are not fully resolved in the subsequent stage, but rather persist and are gradually mitigated amid technological iterations.*

**Figure 2.** The evolution of tree diameter estimation based on terrestrial photogrammetry technology.

The DBH measurement accuracy based on terrestrial photogrammetry technology is significantly constrained by multi-dimensional factors. First, within a reasonable shooting range, the closer the distance between the target and the shooting path, the better the completeness and detail accuracy of point cloud reconstruction [36]. However, excessively close shooting distances will lead to insufficient image overlap and intensified lens distortion, which in turn reduce reconstruction quality. Meanwhile, this technology is highly sensitive to scene texture and illumination conditions [37,38]. When illumination changes drastically or features in overlapping image regions are not significant, it is difficult to extract sufficient matching feature points, which directly affects the reconstruction effect. In addition, image-based point clouds cannot effectively penetrate dense foliage layers, which will significantly reduce the completeness and detail capture capability of trunk reconstruction in forest stands with complex site conditions and severe occlusion [39]. Second, the hardware performance of the acquisition system is the core foundation restricting accuracy. The resolution of the image sensor determines the image detail capture capability and low-light adaptability, while the lens focal length and distortion characteristics affect the stereo-matching accuracy and geometric fidelity of three-dimensional reconstruction. Third, the adaptability of indoor data-processing and algorithm models also significantly affects measurement accuracy. For example, the DBH fitting method proposed by Gao et al. [27] has insufficient applicability to trees with trunks that deviate significantly from a circular shape, resulting in relatively high Root Mean Square Error (RMSE) in their DBH measurement results (Table 1).

**Table 1.** Accuracy comparison table of different algorithms for terrestrial photogrammetry-based DBH estimation.

| Research | Equipment | DBH Retrieval Method | Forest Type | RMSE DBH (cm) * |
|---|---|---|---|---|
| Liang et al. [39] | Samsung NX 300 compact camera (Samsung, Seoul, Republic of Korea) | Cylinder fitting | Mature coniferous and broad-leaved mixed forest | 2.39 |
| Surový et al. [23] | Sony NEX 7 (Sony, Tokyo, Japan) | Stems digitized using magnetic motion tracker | Coniferous and broad-leaved mixed forest | 0.59 |
| Mokroš et al. [24] | Canon 70D (Canon, Tokyo, Japan) | Multi height circle fitting | Coniferous and broad-leaved mixed forest | non-fisheye lens: 0.40–0.67 fisheye lens: 0.38–0.54 |
| Gao et al. [27] | Panasonic DCM-LX7 camera (Panasonic, Osaka, Japan) | Least Median of Squares cylinder fitting | Coniferous forest, deciduous broad-leaved forest | 1.18–3.16 |
| Liu et al. [28] | two CCD lenses (SONY ILCE-QX1, Sony, Tokyo, Japan) | least-squares ellipse fitting | Coniferous and broad-leaved mixed forest | 0.92–1.13 |
| Wu et al. [29] | Android Xiaomi 3 (Xiaomi, Beijing, China) | Adaptive feature coordinate system for DBH measurement | - | 0.217 |
| Fan et al. [30] | Lenovo Phab 2 Pro (Lenovo, Beijing, China) | Levenberg Marquardt + RANSAC circle fitting | Deciduous broad-leaved forest, deciduous coniferous forest | 0.39–2.22 |
| Su et al. [32] | Android smartphone | Circle fitting | Deciduous broad-leaved forest, coniferous forest | 0.46–1.24 |
| Yan et al. [35] | iPad Pro (Apple Inc., Cupertino, CA, USA) | Combined with Image Enhancement and Self-Attention Mechanisms for Improved Point Cloud Quality | Evergreen coniferous and broad-leaved mixed forest, coniferous forest | 0.71–1.16 |

* Results from some studies are presented as ranges, as these studies involved comparisons across multiple tree species, study sites, or analytical methods.

### 3.2. Aerial Photogrammetry

Terrestrial photogrammetry is limited by plot scale and understory operating space, making it difficult to meet the demand for large-area and high-frequency monitoring. Aerial photogrammetry [40] has expanded from close-range individual tree acquisition on the ground to large-scale and rapid acquisition from aerial platforms, satisfying the requirements of large-scale, high-efficiency, and regionalized forest resource inventory. As shown in Figure 3, early aerial photogrammetry mostly indirectly estimated DBH based on the allometric growth relationship between canopy geometric metrics and DBH [41], and direct trunk measurement was only feasible in open forest stands with sparse canopies. With the increasing maturity of SfM-MVS technology, dense point clouds can be generated from multi-view images [42] and fused or compared with an external Digital Terrain Model (DTM) [43,44], enabling automated individual tree localization and canopy parameter extraction at the plot scale. However, under closed canopy conditions, SfM-MVS technology still cannot fundamentally solve the problem of unreliable recovery of DTMs and understory structures [45,46], and the generated trunk point clouds are far inferior to LiDAR point clouds in terms of accuracy and completeness [47,48]. Subsequent related studies have extended modeling features from single canopy geometry to three-dimensional canopy structure and complexity metrics [49–52], and the application of machine learning and deep learning has further improved the stability of tree-crown instance segmentation [53,54].

Aerial photogrammetry has outstanding advantages in cost and deployment flexibility, and can simultaneously preserve image texture and spectral information, providing support for the interpretation and classification of forest elements [55,56]. Nevertheless, its accuracy is affected by multiple factors. First, it is highly sensitive to illumination changes, low-texture areas, and canopy occlusion. Second, aerial photography parameters (flight altitude, camera tilt angle, shooting angle, and image overlap) have a significant impact: lower flight altitudes produce smaller Ground-Sampling Distance (GSD) and more complete and reliable point cloud data [57], and when reasonably combined with multi-angle shooting, higher DBH estimation accuracy can be achieved (e.g., Erfanifard et al. [58] reduced RMSE from 18.30 cm to 2.46 cm after fusing vertical and oblique images, As shown in Table 2). Third, forest stand characteristics (structure, tree species diversity, and canopy closure) are crucial: the high RMSE results in Bennett et al.'s [49] study were primarily caused by the high forest stand structure complexity and tree species diversity in the study area; in contrast, Almeida et al. [50] and Xu et al. [54] both achieved excellent estimation accuracy by relying on sample plot conditions of low canopy closure and unevenly distributed forest stands, combined with robust algorithm design.

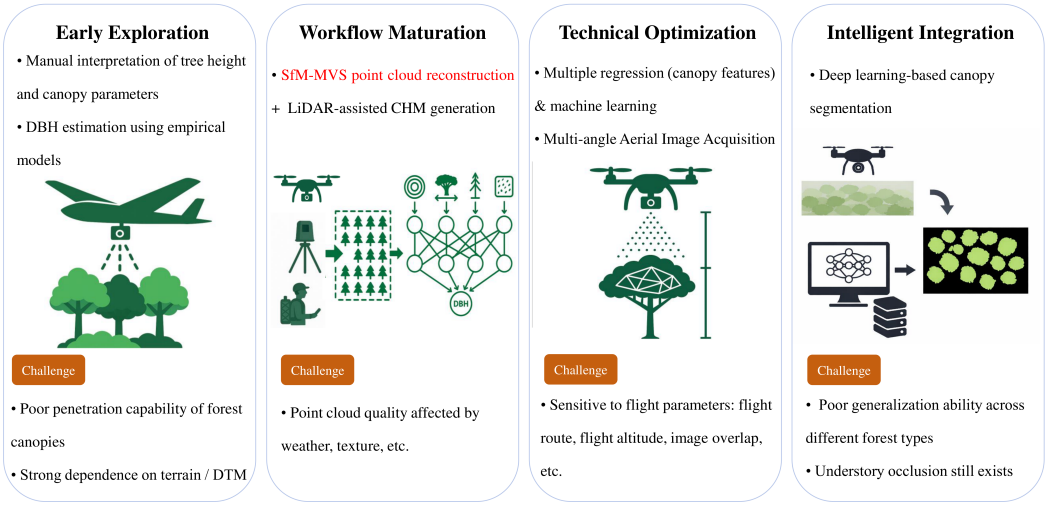



**Figure 3.** The evolution of tree diameter estimation based on aerial photogrammetry technology.

**Table 2.** Accuracy comparison table of different algorithms for aerial photogrammetry-based DBH estimation.

| Research | Equipment | DBH Retrieval Method | Forest Type | RMSE DBH (cm) * |
|---|---|---|---|---|
| Firtz et al. [47] | MK Okto2 (MK Messtechnik, Heidelberg, Germany) + Panasonic Lumix G3 (Panasonic, Osaka, Japan) | RANSAC cylinder fitting | Broad-leaved forest | - |
| Bennett et al. [49] | DJI Phantom 4 advanced (DJI, Shenzhen, China) | Build h-d quantile regression models using external data | Coniferous forest | 4.0–15.1 |
| Almeida et al. [50] | DJI Phantom 4 PRO (DJI, Shenzhen, China) | Fitting regression model using metrics derived from Fourier transforms of profiles | Secondary broad-leaved forest | 0.8 |
| Xu et al. [54] | DJI MAVIC 2 PRO (DJI, Shenzhen, China) | BlendMask segmentation model and a Bayesian neural network for DBH prediction | Coniferous and broad-leaved mixed forest | 0.73 |

**Table 2.** *Cont.*

| Research | Equipment | DBH Retrieval Method | Forest Type | RMSE DBH (cm) * |
|---|---|---|---|---|
| Tinkham et al. [52] | DJI Phantom 4 PRO (DJI, Shenzhen, China) | five model in predicting the missing DBH | Uneven-aged coniferous forest | - |
| Erfanifard et al. [58] | DJI Phantom 4 PRO (DJI, Shenzhen, China) | Least-squares circle fitting | Evergreen coniferous plantation | 2.46–18.30 |

* Results from some studies are presented as ranges, as these studies involved comparisons across multiple tree species, study sites, or analytical methods. The studies by Fritz et al. [47] and Tinkham et al. [52] listed in the table did not report the RMSE for DBH inversion, owing to differences in their research objectives and validation benchmarks.

## 4. DBH Estimation Based on LiDAR Scanning Technology

LiDAR generates high-precision 3D spatial coordinates for each point in space by emitting laser pulses and recording their echo times or phases, providing a non-contact, modeling-capable data foundation for DBH measurement. Compared with imaging-based methods that rely on illumination and texture, LiDAR is less susceptible to performance instability caused by degraded imaging conditions in weak-textured, heavily occluded under-canopy environments. In contrast to traditional contact-based measurements, its advantage does not lie in advancing precision from the centimeter level to the millimeter level, but in providing dense, objective and repeatable trunk cross-sections and stem form curves within an acceptable error tolerance, thereby significantly improving the efficiency of large-sample forest surveys.

### *4.1. Terrestrial Laser Scanning*

Optical photogrammetry is a passive remote sensing technology that relies on natural light reflection for imaging. It is highly sensitive to illumination and texture conditions, and exhibits insufficient stability in DBH reconstruction in forest stands with high canopy closure. In contrast, Terrestrial Laser Scanning (TLS), as an active remote sensing technology, can directly acquire high-density trunk point clouds at the plot scale, and its measurement results have become the accuracy benchmark for non-contact DBH measurement [59–63]. Focusing on the core objectives of automatic extraction of tree positions and DBH in early studies, a series of research works [64–67] gradually established an automated workflow for trunk detection and DBH estimation: point cloud preprocessing → ground point segmentation → trunk extraction → circle fitting at breast height. Subsequent studies have continuously introduced algorithm optimization strategies within this framework to improve the robustness of DBH estimation [68–79] (see Figure 4). To reduce the workload and time cost of manually deploying registration targets in the field and improve point cloud acquisition efficiency, numerous studies have also proposed target-free and target-reduced optimization strategies for multi-station scanning [80,81]. The relevant registration method systems and existing problems of TLS have been systematically summarized in review articles [82,83].

Over the past decade, TLS has undergone continuous advancements in measurement accuracy and applicability for forest sample plot inventory. Of particular note, hardware upgrades and algorithm optimization exert fundamentally distinct driving effects on the iterative refinement of TLS measurement performance, with a clear shift in the core driving force over this period. On the one hand, early-stage accuracy improvements were primarily hardware-driven: iterative hardware advancements primarily improved point cloud density, data acquisition efficiency, and ranging stability, thereby laying a robust data foundation for high-precision forest observation. However, such hardware-centric improvements cannot address the core bottlenecks prevalent in complex forest stands, including point cloud occlusion, noise contamination, and registration misalignment. On the other

hand, algorithm optimization targeting key technical workflows—namely point cloud preprocessing, stem segmentation, DBH circle fitting, and multi-station registration—has emerged as the core driving force behind step-change gains in TLS-based stand parameter estimation accuracy over the past 5 years. This algorithm-driven innovation holds the key to overcoming measurement limitations in complex, high-closure forest stands and enhancing the robustness of forest structural parameter retrieval.

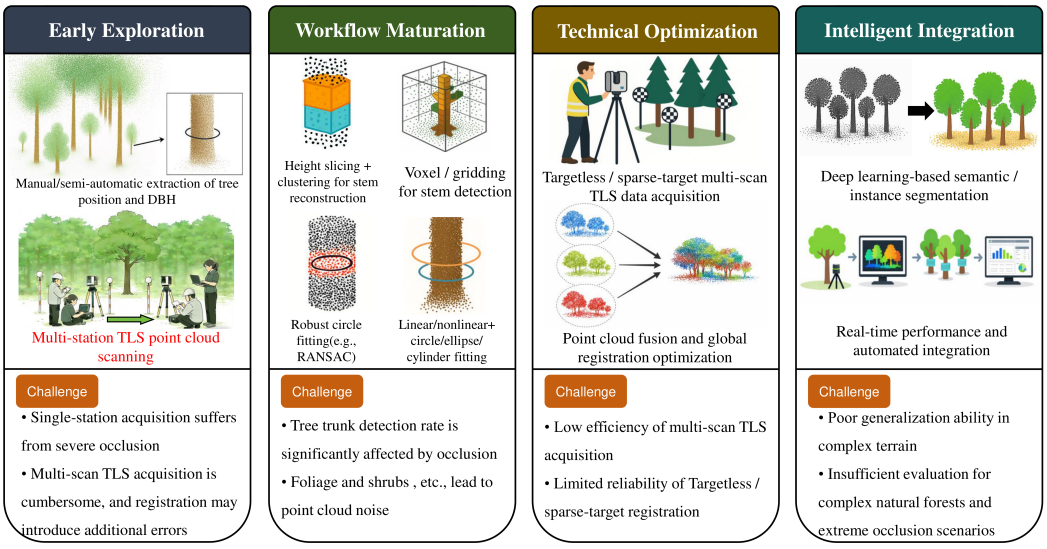



**Figure 4.** The evolution of tree diameter estimation based on Terrestrial Laser Scanning technology.

TLS measurement errors mainly originate from incomplete point cloud cross-sections caused by trunk occlusion, and both scanning distance [84] and station layout schemes also have significant impacts on DBH estimation accuracy: the relatively high RMSE reported by Moskal et al. [85] was mainly attributed to severely twisted and occluded tree trunks in their study plots (see Table 3), limited adaptability of the single-slice cylinder-fitting algorithm to non-ideal trunk morphology, and insufficient point cloud completeness caused by single-station scanning. In contrast, Ritter et al. [86] achieved an overall tree detection accuracy of 97.2% in a structurally complex mature mixed coniferous–broad-leaved stand by adopting a multi-scan scheme. Research by Srinivasan et al. [87] also confirmed that the RMSE of DBH estimation could be reduced from 1.83 cm for single-station scanning to 0.74 cm for dual-station scanning, fully demonstrating the improvement in point cloud completeness via multi-scan deployment. The study area in Liu et al. [88] featured straight trunks with nearly circular cross-sections, providing favorable conditions for DBH extraction using the randomized Hough transform (RHT). Other low-error results were also closely associated with targeted algorithm optimizations, appropriate acquisition schemes, and simple stand structures. Notably, Lee et al. [89] obtained a wide range of RMSE values in the same controlled experiment: higher RMSE values concentrated in single-station scanning scenarios. Among these values, the maximum of 6.52 cm corresponds only to single-station scanning conditions. Measurement accuracy improves significantly with an increasing number of scan stations. When the number of scans increases to 3–5 stations, the RMSE generally falls below 2 cm, and no further significant gain in accuracy is observed with additional scans. The study also pointed out that the selection of the optimal circle-fitting algorithm should match the number of scan stations and the level of data noise. Moreover, in the presence of registration noise, excessive scan positions and overly high point cloud density may reduce DBH measurement accuracy.

**Table 3.** Accuracy comparison table of different algorithms for TLS-based DBH estimation.

| Research | Equipment | DBH Retrieval Method | Forest Type | RMSE DBH (cm) * |
|---|---|---|---|---|
| Moskal et al. [85] | Leica HDS 3000$^{TM}$ (Leica, San Ramon, CA, USA) | Least-squares cylinder fitting | Deciduous forest, mixed forest, coniferous forest | 9.17 |
| Ritter et al. [86] | FARO Focus3D X330 (FARO, Lake Mary, FL, USA) | Least-squares circle/ellipse fitting | Mature coniferous and broad-leaved mixed forest | 4.95 |
| Li et al. [90] | Riegl VZ-400 (Riegl, Horn, Austria) | 2D Hough transform and ellipse fittingh | Deciduous broad-leaved forest | 1.92–3.58 |
| Bu et al. [91] | Riegl VZ-400 (Riegl, Horn, Austria) | Adaptive circle–ellipse fitting | Deciduous broad-leaved forest | 1.99 |
| Zheng et al. [92] | FARO Focus3D X130 (FARO, Lake Mary, FL, USA) | Hough transform DBH estimation | Secondary deciduous broad-leaved forest | 2.03 |
| Srinivasan et al. [87] | Leica ScanStation2 (Leica, Heerbrugg, Switzerland) | Cylinder fitting | Deciduous broad-leaved forest, evergreen coniferous forest | 0.74 |
| Liu et al. [88] | Leica P40 (Leica, Heerbrugg, Switzerland) | random Hough transform DBH estimation | Coniferous forest | 0.68–1.64 |
| Lee et al. [89] | Leica BLK 360 (Leica, Heerbrugg, Switzerland) | Least-squares circle/ellipse (RANSAC) fitting | Evergreen coniferous plantation, deciduous coniferous plantation | 0.97–6.52 |

* Results from some studies are presented as ranges, as these studies involved comparisons across multiple tree species, study sites, or analytical methods.

### *4.2. Handheld Mobile Laser Scanning*

Static multi-station scanning mode of TLS suffers from cumbersome deployment and limited maneuverability, making it difficult to meet the requirements for efficient investigation of large sample plots. Compared with high-precision TLS systems, mobile laser scanning features significantly lower equipment procurement and field operation costs, demonstrating outstanding cost-effectiveness in large-scale forest resource surveys. It requires no complex base-station setup or flight-path planning, and a single operator can complete the whole process of under-canopy data acquisition, with an operational threshold much lower than that of similar laser scanning equipment. However, its point cloud quality and measurement accuracy highly depend on the operator's work specifications and path design, resulting in a clear trade-off between operational convenience and result accuracy. Handheld Mobile Laser Scanning (HMLS) shows great potential in rapidly acquiring point clouds and key structural parameters over large areas due to its high maneuverability and efficient data collection capability, while also facing technical challenges such as algorithm robustness, environmental occlusion, and positioning drift [93,94].

As shown in Figure 5, early HMLS systems typically consisted of low-cost laser scanners and Inertial Measurement Units (IMU). In forest environments, Global Navigation Satellite System (GNSS) signals degrade due to canopy occlusion, rendering GNSS-based positioning unreliable. To overcome this bottleneck, researchers introduced Simultaneous Localization and Mapping (SLAM) algorithms into HMLS systems to replace GNSS as the core pose estimation solution in signal-deprived environments. By jointly processing laser data and IMU observations, SLAM algorithms can estimate the scanner trajectory and register point clouds in unknown environments [95–98], marking a key turning point for the practical application of HMLS technology in forest surveys and enabling HMLS to perform well in DBH estimation in most forest scenarios [99–105].

The DBH measurement accuracy based on HMLS is constrained by multiple factors. From the dimension of forest stand characteristics, the study areas of both Ryding et al. [106]

and Gollob et al. [107] were complex forest stands with dense vegetation. Combined with the performance limitations of early instruments (point density, angular resolution, etc., which were far lower than those of TLS systems), both studies obtained relatively high RMSE values (Table 4). Yang et al. [108] further confirmed that forest stand type and topographic conditions have significant impacts on the DBH measurement accuracy of HMLS. Among them, trunk inclination, irregular trunk cross-sections, and forest stand occlusion are the core error sources, and the effects of these factors are more pronounced in coniferous forest scenarios. From the dimension of algorithms and data-processing workflows, the robustness of SLAM algorithms, point cloud registration strategies, trunk point cloud segmentation, and DBH extraction algorithms are the core variables determining the final measurement accuracy. Pose estimation errors of SLAM algorithms directly lead to point cloud registration misalignment and trunk contour deformation, which are the core sources of localization drift during long-distance understory scanning. The selection of registration strategies in the data-processing workflow directly regulates the final accuracy of DBH estimation: Tupinambá-Simões et al. [109] compared the performance of two registration modes in the HMLS 3D point cloud generation process, and the rigid registration mode generally yielded higher RMSE across different sample plots and tree species. In addition, operational specifications such as the operator's scanning path design [110], operating speed, and point cloud overlap control directly affect the pose estimation accuracy of SLAM algorithms and the effect of point cloud registration.

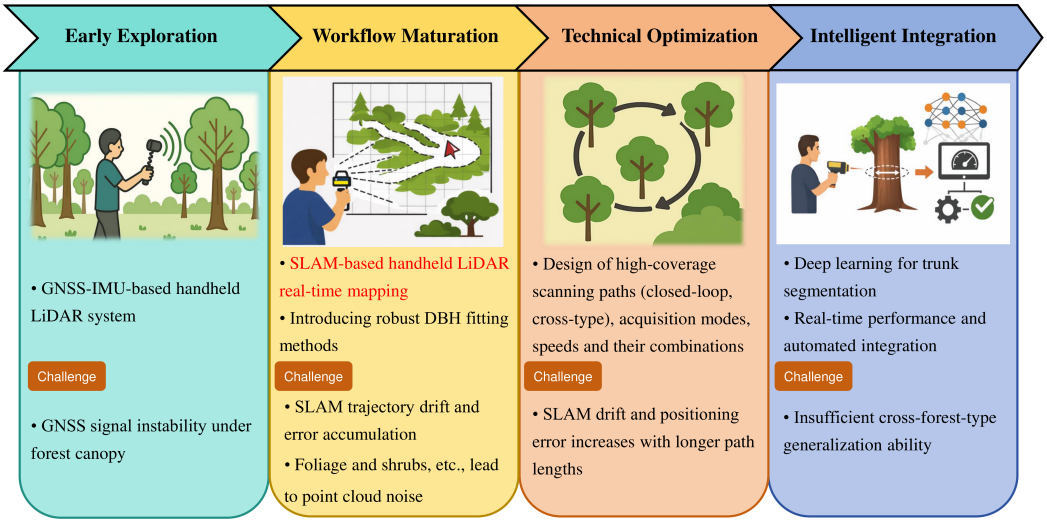



**Figure 5.** The evolution of tree diameter estimation based on Handheld Mobile Laser Scanning technology.

**Table 4.** Accuracy comparison table of different algorithms for HMLS-based DBH estimation.

| Research | Equipment | DBH Retrieval Method | Forest Type | RMSE DBH (cm) * |
|---|---|---|---|---|
| Ryding et al. [106] | ZEB1 (GeoSLAM, Nottingham, UK) | Cylinder fitting | Deciduous broad-leaved forest | 2.9 |
| Bauwens et al. [111] | ZEB1 (GeoSLAM, Nottingham, UK) | Least-squares circle fitting | Deciduous forest, mixed forest, coniferous forest | 1.11 |
| Gollob et al. [107] | ZEB-HORIZON (GeoSLAM, Nottingham, UK) | Multi layer cross-section circle/ellipse/spline combination fitting | Deciduous forest, mixed forest, coniferous forest | 2.56–3.32 |

**Table 4.** *Cont.*

| Research | Equipment | DBH Retrieval Method | Forest Type | RMSE DBH (cm) * |
|---|---|---|---|---|
| Tupinambá-Simões et al. [109] | ZEB-HORIZON (GeoSLAM, Nottingham, UK) | Cylinder fitting | Coniferous and broad-leaved mixed forest | 1.44–7.85 |
| Zhou et al. [112] | Velodyne VLP-16 (Velodyne, San Jose, CA, USA) | RANSAC circle fitting | Broad-leaved plantation | 0.70–1.18 |
| Proudman et al. [113] | Ouster OS0-128 LiDAR (Ouster, San Francisco, CA, USA) | RANSAC circle fitting | broad-leaved forest | 5.6 |
| Yang et al. [108] | LiGrip H120 (GreenValley, Beijing, China) | Cylinder fitting | Coniferous and broad-leaved mixed forest | 1.26–2.79 |

* Results from some studies are presented as ranges, as these studies involved comparisons across multiple tree species, study sites, or analytical methods.

### *4.3. Backpack Laser Scanning*

HMLS is affected by the operator's grip posture, resulting in unstable scanning trajectories and significant cumulative SLAM drift errors over long-distance operations, making it difficult to support long-range, large-scale continuous forest surveys. Backpack Laser Scanning (BPLS) offers higher operational stability compared to HMLS. Its backpack design is more ergonomic, effectively reducing operator fatigue and improving terrain adaptability, allowing BPLS to balance operational efficiency and data quality in large-scale forest surveys over complex terrain. It has thus become an important complementary form of ground-based laser scanning technology in forestry applications.

Early studies on individual tree DBH estimation using BPLS primarily validated its feasibility at the plot scale [114]. However, due to limitations such as sensitivity to noise, insufficient single-trajectory data coverage, and simplistic geometric fitting methods, BPLS was prone to omission and misfitting in complex stands. Subsequent research has progressively improved the technology from three perspectives (Figure 6): First, a fusion strategy combining multi-scan and circle fitting [115,116] effectively reduced the impact of positioning errors on DBH estimation, but stability remains insufficient in extremely weak signal environments. Second, a dual-scanner configuration [117] (horizontal and vertical scanners operating collaboratively), coupled with the iterative closest point (ICP) algorithm, improved positional accuracy, yet tended to generate many false trees in dense forest areas. Third, initial trajectory estimation using GNSS/IMU combined with SLAM backend optimization enabled real-time correction of positioning drift [118], achieving DBH estimation accuracy close to that of Terrestrial Laser Scanning in simple plots, but recognition of small or irregular trees in complex stands remained challenging. In recent years, research has further focused on algorithmic refinements, such as intensity filtering, cluster analysis, and point cloud density correction [119–122], bringing DBH estimation errors within the centimeter level.

Overall (see Table 5), BPLS has achieved centimeter-level accuracy under certain stand conditions through improved hardware configuration, trajectory optimization, and multi-source data fusion. However, this method still struggles with stem inclination or irregular morphology, limiting its generalization in complex stands. Future research on BPLS should focus on adaptive modeling of stem shape and lightweight algorithm design to enhance its applicability in complex ecological environments.

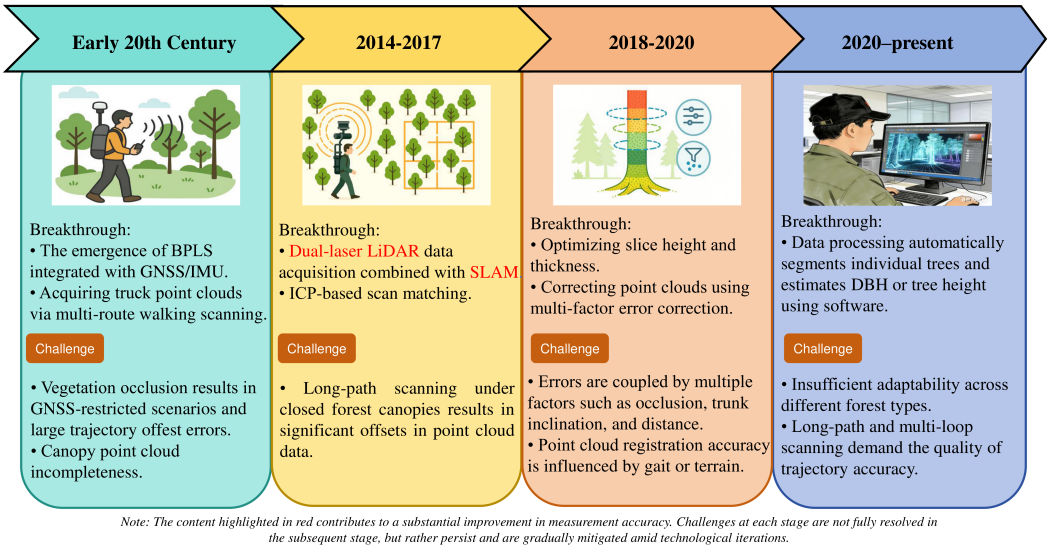



**Figure 6.** The evolution of tree diameter estimation based on Backpack Laser Scanning technology.

**Table 5.** Accuracy comparison table of different algorithms for BPLS-based DBH estimation.

| Research | Equipment | DBH Retrieval Method | Forest Type | RMSE DBH (cm) * |
|---|---|---|---|---|
| Liang et al. [114] | AKHKA R2 (Finnish Geodetic Institute, Masala, Finland) | A multipass-corridor-mapping approach/cylinder fitting | Mature forest | 5.06 |
| Holmgren et al. [115] | An in-house BPLS system (Velodyne LiDAR, CA, USA) | Dynamic calibration/PCA-based stem axis estimation/circle fitting | Mature forest | 1.9 |
| Oveland et al. [117] | An in-house dual-scanner BPLS system (Velodyne LiDAR, CA, USA) | Trunk center point registration based on the ICP algorithm/circle fitting | Boreal forest | 2.2 |
| Hyyppä et al. [118] | AKHKA R3 (Finnish Geodetic Institute, Masala, Finland) | Graph SLAM optimization/Scanning Line Arc Extraction and Matching/Algebraic Fitting | Boreal forest | Easy plot: 1.2<br>Medium plot: 1.7 |
| Huang et al. [119] | Li Backpack 50 (Green Valley, Beijing, China) | Lidar360 (V2. 2) | Secondary deciduous broad-leaved mixed forest and artificial coniferous forest | Different Plots: 0.60–1.92 |
| Cai et al. [120] | Backpack SLAM 3D scanning system | Landou-Smith circle fitting algorithm | Sparse plantation | Flat ground: 0.99;<br>Gentle slope: 4.72;<br>Steep slope: 2.15 |
| Xie et al. [122] | LiBackpack D-50 (Green Valley, Beijing, China) | Improved Progressive TIN Densification Algorithm/Cylinder Fitting Based on 3D Least Squares | Artificial coniferous forest | 2.09 |

* Results from some studies are presented as ranges, as these studies involved comparisons across multiple tree species, study sites, or analytical methods.

### *4.4. UAV-Borne LiDAR*

Although near-ground laser scanning (TLS, HMLS, BPLS) can acquire high-precision stem point clouds, its plot-scale coverage is limited, making it difficult to support large-area forest resource monitoring. Airborne laser scanning, deployed on UAV or manned aircraft platforms, enables two observation modes: above-canopy and under-canopy. These correspond to different priorities—efficiency for large-area coverage versus geometric

accuracy for fine-scale details. The two approaches have their respective advantages and disadvantages, and are suited to different application scenarios [123–125].

#### 4.4.1. Above-Canopy ULS System

In early studies, above-canopy ULS was primarily constrained by two major bottlenecks: first, insufficient positioning and orientation accuracy. Due to payload limitations, UAV positioning and orientation systems had to strike a balance between accuracy and weight, and even minor positional errors could lead to significant point cloud misalignment [126]. Second, DBH estimation faces the problem of missing point cloud data at breast height. Although Jaakkola et al. [127] and Wallace et al. [128] have demonstrated the potential of above-canopy ULS for DBH estimation from the perspectives of system integration and trajectory solution, respectively, under above-canopy observation conditions, the point cloud of the trunk at breast height is difficult to obtain, forcing DBH to rely either on coarse geometric fitting or on indirect inference primarily based on canopy information.

To overcome the above bottlenecks, the technological evolution has gradually formed three main lines (Figure 7). The first main line [129] shifted from directly fitting the stem point cloud to robust estimation using canopy features combined with random forest models, which alleviated the problem of insufficient point clouds to a certain extent. The second main line [130] shifted from raster-based individual tree detection (ITD) [131] to point-cloud-based ITD [132], significantly improving DBH prediction accuracy. However, in dense stands, point cloud quality remains the key factor limiting measurement accuracy. The third main line [133] involves acquiring high-density point clouds via high-overlap flight routes, followed by density equalization and sparsification [134]. Studies have found that accuracy is optimal at a point density of approximately 12,200 points/m$^2$, and canopy volume features have repeatedly been confirmed as key variables.

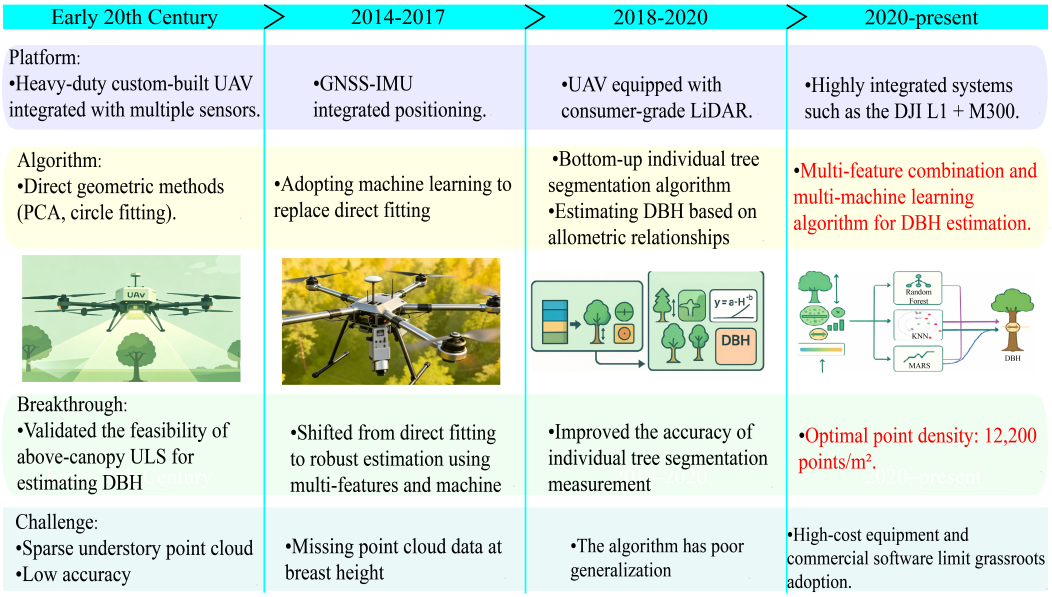



**Figure 7.** The evolution of tree diameter estimation based on above-canopy ULS system. Note: The content highlighted in red contributes to a substantial improvement in measurement accuracy. Challenges at each stage are not fully resolved in the subsequent stage, but rather persist and are gradually mitigated amid technological iterations.

Among the three main lines described above, the path based on machine learning and multi-feature fusion has been the most actively developed, with related research further focusing on the optimization of feature combinations and the comparison of model performance. In terms of feature combination and model selection, the combination of

multiple features (e.g., tree height, canopy density [135], canopy volume, etc.) outperforms a single variable [136], among which the Random Forest [137] model demonstrates the best overall performance. In terms of practical inventory applicability, DBH estimated by above-canopy ULS shows no significant difference from field measurements in middle-aged to mature forests [138]. However, in young and dense stands, certain limitations remain due to difficulties in individual tree identification.

Overall (see Table 6), existing studies have gradually improved the accuracy of above-canopy ULS-derived DBH through improved sensor configurations, optimized point-cloud-processing algorithms, multi-feature combinations, and the introduction of various machine learning models. However, the recognition capability of this technology remains limited in complex and dense forests [139,140]. Moreover, most studies rely on high-cost equipment and commercial software, which restricts its widespread application in grassroots-level forest inventories.

**Table 6.** Accuracy comparison table of different algorithms for above-canopy ULS-based DBH estimation.

| Research | Equipment | Flight Altitude | DBH Retrieval Method | Forest Type | RMSE DBH (cm) * |
|---|---|---|---|---|---|
| Jaakkola et al. [129] | Velodyne Puck LITE (Velodyne LiDAR, CA, USA) | 40 m | DBH estimation via RF, PCA and circle fitting | Coniferous forest | 2.55; 6.82; 5.52 |
| Vandendaele et al. [130] | Velodyne HDL-32E (Velodyne LiDAR, CA, USA) | 40 m | Predicting DBH using height and CD allometry fromraster- or point-cloud-based ITD/cylinder fitting | Naturally grown hardwood | 11.5; 7.3; 7.4 |
| Watt et al. [133] | DJI-Zenmuse L1 (DJI, Shenzhen, China) | 55 m | Predicting DBH using PLS and RF | Radiata pine plantation | 1.624 (PLS was optimal; optimal point density: 12,200 pts/$m^2$) |
| Tang et al. [136] | DJI Zenmuse L1 (DJI, Shenzhen, China) | 80 m | DBH estimation using seven predictive models | Mixed coniferous and broad-leaved forest | 2.371 (Optimal combination: Height, density, canopy traits + RF) |

* Results from some studies are presented as ranges, as these studies involved comparisons across multiple tree species, study sites, or analytical methods.

#### 4.4.2. Under-Canopy ULS System

Under-canopy ULS directly acquires high-resolution point clouds of tree trunks under near-ground conditions, which is more conducive to accurate geometric reconstruction and is particularly suitable for complex environments such as dense canopies. The development of this technology has gone through four stages (Figure 8): In the early stage, 2D LiDAR combined with pattern matching was used to verify feasibility [141], but positioning errors and battery life were prominent issues. Subsequently, SLAM was introduced and combined with 3D LiDAR [142], significantly improving positioning accuracy and the ability to extract trunk arcs, although problems such as incomplete path coverage and reliance on manual operation remained. To address coverage insufficiency, a hybrid scanning strategy combining above-canopy and under-canopy scans along with 360° rotational scanning was proposed [143], effectively improving the completeness of trunk circumferential observations, but platform stability and operator involvement remained limiting factors. The latest advances employ fully autonomous flight [144] and real-time SLAM [145], demonstrating that full-coverage flight paths can reduce positioning errors, but DBH estimation accuracy remains low (RMSE approximately 5 cm). This is due to the combined effect of the limited accuracy of consumer-grade LiDAR hardware, the insufficient stability of the drone platform, the insufficient coverage of some trajectories resulting in excessive distance between the target and the sensor, and the complex forest conditions.

In summary, the core advantage of the above-canopy ULS lies in its coverage efficiency and canopy structure characterization. When the tree trunk is difficult to observe directly, it can make robust indirect inferences based on tree height or canopy features. The under-canopy ULS, on the other hand, excels in short-range tree trunk geometry reconstruction. In environments where GNSS is limited and occlusion is complex, it can easily obtain high-precision DBH by relying on SLAM and robust fitting (Table 7). The recent development trend of the ULS-DBH technology is the coordinated advancement of sensor capabilities and observation design, SLAM, and automated processing: the above-canopy approach enhances the stability of indirect estimation through more refined ITD, canopy features, and high-density sampling, but its upper limit is constrained by the visibility of the tree trunk at breast height; the under-canopy approach improves the completeness of the tree trunk point cloud coverage through SLAM and autonomous navigation, supplemented by collaborative scanning and supplementary scanning strategies. Looking ahead, by improving point cloud quality, optimizing scanning strategies, and enhancing system autonomy and stability, DBH can be measured efficiently and accurately in complex environments, playing a greater role in forest resource surveys.

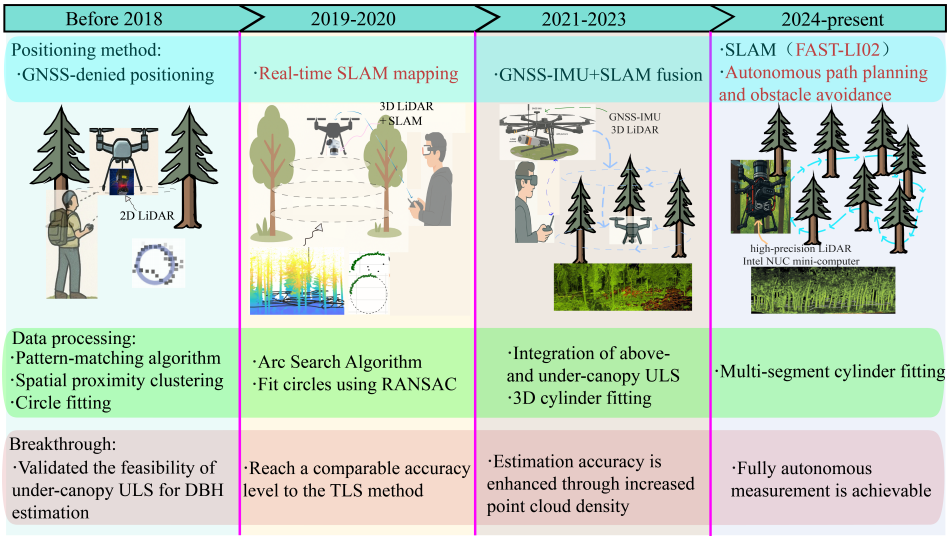



**Figure 8.** The evolution of tree diameter estimation based on under-canopy ULS system. Note: The content highlighted in red contributes to a substantial improvement in measurement accuracy.

**Table 7.** Accuracy comparison table of different algorithms for under-canopy ULS-based DBH estimation.

| Research | Equipment | Flight Altitude | DBH Retrieval Method | Forest Type | RMSE DBH (cm) * |
|---|---|---|---|---|---|
| Chisholm et al. [141] | Hokuyo UTM-30LX LiDAR (Hokuyo Automatic, Osaka, Japan) | 1.5 m | Identifying tree stems via spatial proximity clustering; circle fitting | Casuarina plantation | - |
| Hyyppä et al. [142] | Velodyne VLP-16 (Velodyne LiDAR, CA, USA) | Manual operation under the forest canopy | Arc-Matching and Arc Extraction Algorithm; circle fitting based on RANSAC | Boreal forest | Easy plot: 0.69; Medium plot: 0.92 |
| Wang et al. [143] | Riegl miniVUX (Tarot Aviation Technology, Wenzhou, China) | 50 m + 1.5 m | 3D cylinder fitting | Boreal forest | The effective area: 3.76 |
| Liang et al. [145] | Self-developed compact quadrotor + Ouster OS1-128 LiDAR (Ouster, San Francisco, CA, USA) | Autonomous under-canopy ULS flights: 1.8 m | Least squares circle fitting | Typical single-layer managed forest | 5.13 |

* Results from some studies are presented as ranges, as these studies involved comparisons across multiple tree species, study sites, or analytical methods.

## 5. Applications of Multi-Source Sensor Fusion in Forest DBH Estimation

Single-sensor platforms have inherent observational limitations in the remote sensing inversion of forest structural parameters: TLS can measure DBH with high accuracy, but it is difficult to conduct large-scale surveys and suffers from missing upper-canopy information; aerial platforms can achieve full-coverage observation of canopies at large scales, but they struggle to penetrate dense canopies to obtain geometric information of lower trunks, which directly constrains the upper limit of DBH inversion accuracy. To address these technical bottlenecks, multi-sensor data fusion technology (Figure 9) achieves complementary advantages by integrating heterogeneous data from different platforms [146], thereby enhancing the completeness and application potential of datasets. According to the information processing stage, existing multi-sensor fusion technologies can be divided into three levels: data-level, feature-level, and decision-level fusion [147–149].

Data-level fusion is the lowest-level fusion method for multi-source data. It performs high-precision spatial registration and geometric merging of raw data from different sensors during the preprocessing stage to generate a comprehensive dataset with complete information and strong geometric consistency, providing a three-dimensional geometric foundation for DBH feature extraction and parameter inversion. Its core purpose is to compensate for the perspective differences and information blind spots of heterogeneous platforms, complement the observational advantages of terrestrial and aerial platforms, construct complete 3D point cloud models of individual trees [150,151], and fundamentally resolve DBH extraction errors caused by incomplete point clouds from a single platform. Feature-level fusion does not directly operate on raw data. It first independently extracts feature variables with clear physical meanings from different data sources, then completes screening, combination, and optimization in the feature space. It can adaptively integrate the advantageous features of multiple sensors, compensate for the insufficient feature dimensionality of a single data source, and effectively improve the accuracy and dimensionality of DBH and multi-parameter collaborative inversion [152]. Decision-level fusion allows different sensors to independently complete data processing, target recognition, and preliminary decisions, and then comprehensively optimizes the multi-source preliminary results through specific decision rules. Compared with the previous two levels, it has the lowest requirements for sensor spatiotemporal registration and the strongest environmental interference resistance. It can significantly reduce the false-positive and false-negative rates of trunk detection and automatic DBH identification in complex field scenarios through cross-validation of multi-source results, generate final results with high robustness, and provide stable technical support for automated DBH measurement [153].

Although multi-source fusion technology can indeed break through the limitations of single sensors under specific conditions (complete equipment, algorithm adaptation, and controllable scenarios), its status as a universal solution has not yet been established. For operational applications, this technology still faces four core challenges: cost–benefit imbalance restricts grassroots promotion; inconsistent standard systems make research results difficult to reuse; research on full-chain error propagation and uncertainty quantification is insufficient; and validation in complex mixed forests in tropical and subtropical regions is severely lacking. Among these challenges, the high equipment cost and complex system design of platform-level multi-source fusion technology have become prominent bottlenecks restricting its large-scale popularization and application in routine forest inventory. To address this issue, researchers have begun to explore consumer-grade mobile platforms as low-cost and high-efficiency alternatives for DBH measurement. Arunima Singh et al. [154] achieved centimeter-level measurement accuracy (RMSE $\approx$ 2.58 cm) using an iPhone 12 Pro, while Xiang Wang et al. [155] further optimized the DBH estimation method for the iPhone 13 Pro, improving the measurement accuracy to RMSE $\approx$ 0.63 cm. Consumer-grade

mobile platforms integrated with smartphone LiDAR combine the advantages of low cost, low technical threshold, and high operational efficiency. They are particularly suitable for survey scenarios where obtaining core DBH parameters is the primary objective and comprehensive reconstruction of tree structures is not required, laying a foundation for the daily application of DBH measurement technologies.

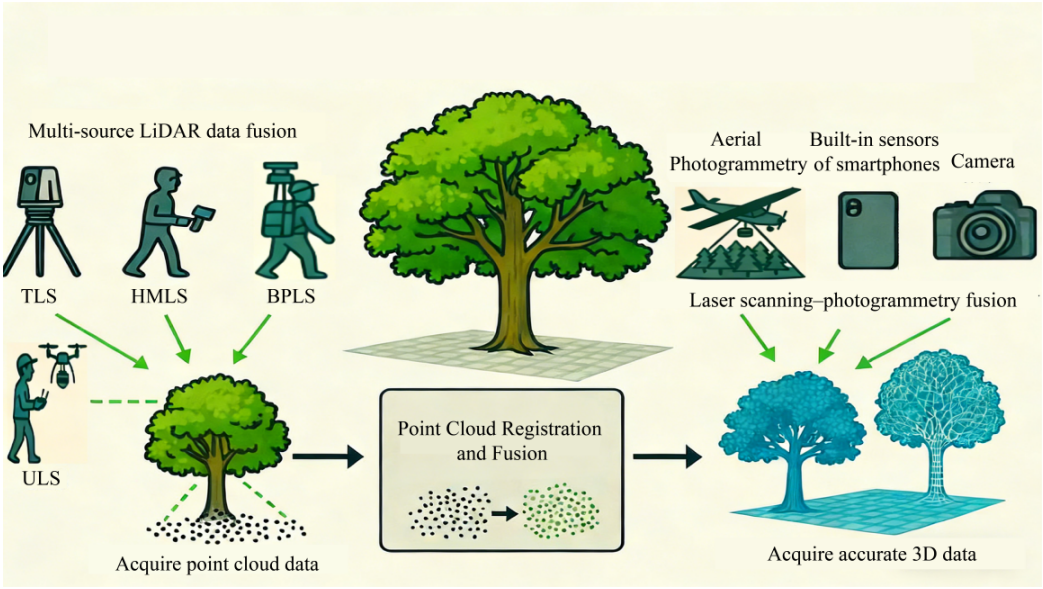



**Figure 9.** 3D tree data acquisition by multi-source LiDAR and photogrammetry fusion.

Future research should focus on four directions: establishing a unified fusion standard system and open-source toolchains; conducting full-chain error propagation modeling; strengthening field validation in complex forest stands; and promoting the deep integration of fusion algorithms with lightweight edge computing.

## 6. Comprehensive Evaluation and Decision Framework for DBH Measurement Techniques

### *6.1. Multi-Dimensional Comprehensive Evaluation of DBH Measurement Technologies*

This section conducts a multi-dimensional horizontal comparison of mainstream DBH measurement technologies based on field measurement results from the published literature and engineering application feedback (Table 8), and constructs a radar chart of comprehensive technical performance based on a five-dimensional evaluation system (Figure 10). Except for traditional non-contact measurement methods that use absolute error, all other technologies adopt RMSE (cm) as the core accuracy evaluation metric. The data in the table are all derived from field measurement results of sample plots from the references cited in this paper. Accuracy variations are affected by multiple factors including forest stand characteristics, equipment performance, and algorithm design. Some instrument measurements may be questioned by manufacturers due to inconsistencies between test conditions and the official specifications provided by the manufacturers. The measured extreme values only provide reference for technology selection and do not represent the inherent upper and lower accuracy limits of the technologies.

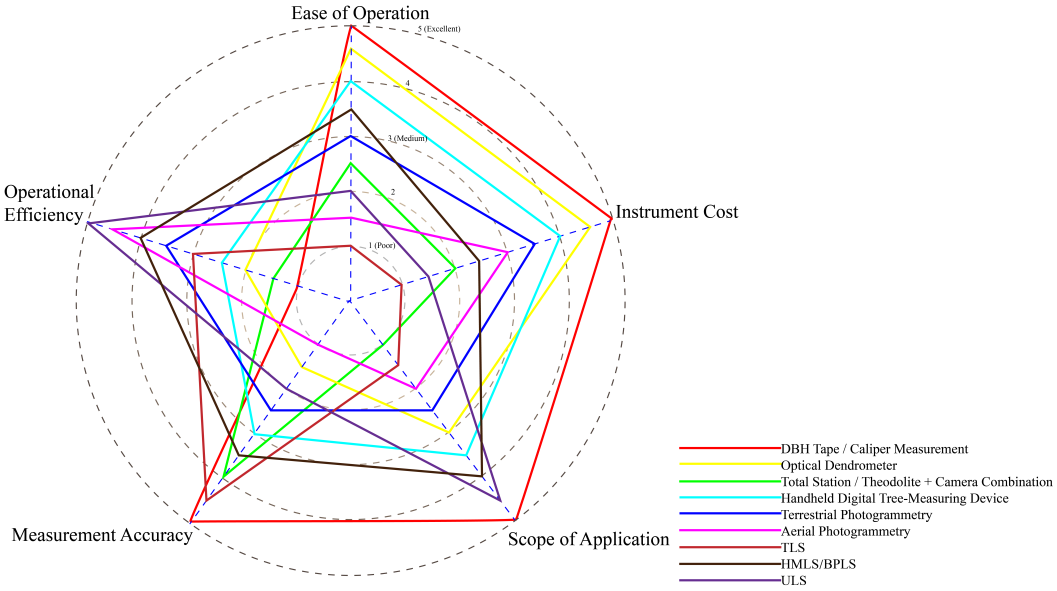



**Figure 10.** Radar chart for multi-dimensional evaluation of different DBH measurement techniques.

**Table 8.** Comprehensive comparison table of DBH measurement technologies.

| Method | Advantages | Disadvantages | Applicable Conditions | Application Scope | Instrument Cost | Operational Complexity | Operational Efficiency | RMSE DBH (cm) |
|---|---|---|---|---|---|---|---|---|
| DBH tape/Caliper | Extremely low cost, simple operation, good measurement repeatability | Requires manual contact with the trunk | No strict environmental limitations | Long-term monitoring of individual trees in small plots across various stand types | Extremely low | Simple | Low, tree-by-tree contact measurement | - |
| Optical dendrometer | Simple and durable machine structure | Poor result stability | Adequate lighting, no obstruction at breast height | Simple surveys in small plots within open stands | Low to medium | Low to medium | Low, tree-by-tree aiming and reading | 0.50–2.00 |
| Total station/Theodolite combined with camera | Capable of acquiring multiple parameters | Bulky equipment, complicated operation | Gentle terrain, no obstruction at breast height | High-precision control measurements in small to medium plots | Medium to high | Medium to high, specialized training required for instrument operation | Low, time-consuming setup and calibration | 0.14–2.00 |
| Handheld digital tree measurement device | Portable, simple to operate, strong environmental adaptability | Limited battery life | No obstruction at breast height, good accessibility | Rapid surveys in small to medium plots | Low to medium | Low to medium, no manual reading or calculation required | Medium, rapid tree-by-tree reading | 0.17–2.50 |
| Terrestrial photogrammetry | Images contain texture and color information | Dependent on lighting and trunk texture | Uniform lighting, clear trunk texture, weak occlusion | Medium-scale surveys in small to medium plots | Low to medium | Medium, image & point cloud processing | Medium, time-consuming office processing | 0.22–3.16 |
| Aerial photogrammetry | Large-area rapid coverage, providing both geometric and spectral information | Dependent on under-canopy visibility | Sunny weather, weak canopy occlusion | Large-scale forest resource surveys | Medium to high | High, UAV piloting is required; image & point cloud processing | Extremely high, large-area image acquisition | 0.53–5.6 |
| TLS | Benchmark for non-contact measurement accuracy, enabling precise reconstruction of trunk structure | Complex operational workflow | Intervisibility between stations, gentle terrain | Medium-scale high-precision plot surveys | High | High, survey station planning; process point cloud data | Medium, time-consuming multi-station setup and data fusion | 0.97–2.45 |
| HMLS | Highly portable, flexible and efficient for fieldwork | Accuracy depends on SLAM algorithms | Forest areas suitable for continuous walking under favorable weather conditions | Rapid plot surveys in medium-scale stands and forest areas with complex terrain | Medium to high | Medium, fieldwork is convenient; process point cloud data | High, continuous walking-based acquisition | 0.70–7.85 |
| BPLS | Greater stability than HMLS, balancing accuracy and operational scale | | | | | | | 0.60–5.06 |
| above-canopy ULS | Large coverage area and high efficiency | Missing point cloud data at breast height | Sunny weather, weak canopy occlusion | Large-scale, broad-area forest resource inventories | High | High, UAV piloting is required; process point cloud data | Extremely high | 1.62–11.50 |
| under-canopy ULS | Close-range acquisition of high-resolution point clouds | Challenging SLAM-based positioning, short battery life | | | | | | 1.69–5.13 |
| Multi-source data fusion techniques | Effectively compensates for the limitations of single-sensor technologies | Complex multi-platform collaborative workflow | - | Large-scale, multi-scale, full-stand resource inventories | - | Extremely high, requiring cross-disciplinary expertise | Medium, multi-platform coordination, complex workflow | - |

The comprehensive comparison demonstrates that no DBH measurement technology has absolute advantages or disadvantages, and the core of their application value lies in their adaptability to specific survey scenarios. Traditional contact measurement is the universally recognized benchmark for accuracy verification, with strong environmental adaptability and low operational thresholds, but it suffers from insufficient efficiency and is only suitable for small-scale benchmark monitoring. Traditional non-contact measurement breaks through spatial constraints, but exhibits inadequate stability in complex forest stands and is mostly used as an auxiliary means for simple surveys. Modern photogrammetric technology features low cost, rich information content, and wide coverage scales, but is highly sensitive to illumination and occlusion, and only yields stable results under controllable environmental conditions. LiDAR technology overcomes the environmental limitations of passive optical technologies through active detection. Among them, TLS serves as the accuracy benchmark for non-contact measurement, HMLS/BPLS strikes a balance among accuracy, efficiency, and portability, and ULS can meet the coverage requirements of large-scale surveys.

### *6.2. An Engineering Practice-Oriented Decision Framework for Technology Selection*

Based on the aforementioned multi-dimensional comprehensive evaluation results, the core of DBH measurement technology selection is not to pursue optimal performance in a single dimension, but to achieve precise matching among survey requirements, scenario constraints, and technical capabilities. Accordingly, this section constructs a hierarchical technology selection decision tree (Figure 11) with survey scale as the primary decision node, site and forest stand conditions as the secondary decision nodes, and accuracy requirements as the tertiary decision node, providing reference guidance for technology selection in the engineering practice of forest inventory.

The core of technology pathway elimination in this decision system is based on three major constraints: mismatch between performance and core scenario requirements, conflict between applicable conditions and environmental constraints, and discrepancy between engineering thresholds and implementation conditions. For different survey scales, the system defines differentiated selection logics: small-scale scenarios prioritize measurement stability and repeatability, eliminating large-scale coverage aerial technologies to avoid cost–benefit imbalance; in sub-scenarios with steep slopes and dense forest stands, passive optical technologies that are significantly affected by the environment are excluded; medium-scale scenarios focus on the comprehensive balance between accuracy and efficiency, allowing for flexible selection based on site conditions, accuracy requirements, and cost budgets; large-scale scenarios prioritize wide-area coverage and operational efficiency, thus eliminating all ground-based individual-tree measurement technologies, including both contact and near-ground non-contact methods.

This system clarifies the application boundaries and scenario-based selection logic of DBH measurement technologies, providing a reference for technology selection in forestry inventory. In practical applications, flexible selection should be made according to on-site conditions, and multi-technology fusion can also be adopted to compensate for the shortcomings of single technologies, achieving the optimal balance among accuracy, efficiency, and cost.




**Figure 11.** A decision tree for selecting DBH measurement techniques based on survey scale and topographic conditions.

## 7. Conclusions and Future Directions

DBH measurement technology has undergone a paradigm shift from contact single-tree measurement to non-contact measurement, and then to multi-platform, multi-scale, and automated measurement. This paper systematically reviews this evolution process, and for the first time reveals the internal driving force of technology iteration from the three core contradictions of accuracy and efficiency, cost and coverage, and manual and automation. It builds a multi-dimensional comprehensive evaluation system and a three-level decision tree of "survey scale–site conditions–accuracy requirements", providing quantitative basis for technology selection; and focuses on analyzing the implementation paths and key challenges of multi-source fusion technologies (data level, feature level, decision level).

To meet the new requirements for data accuracy, coverage, and timeliness under the carbon neutrality goals, and to overcome current technological application bottlenecks, this paper proposes short-, medium-, and long-term development and promotion recommendations: In the short term, promote low-cost mobile scanning devices such as handheld/backpack LiDAR and smartphone-integrated LiDAR, develop user-friendly data-processing software, and strengthen grassroots personnel training to achieve technological upgrades at the grassroots level. In the medium term, establish multi-source data fusion standards, promote cross-regional and cross-sectoral data sharing, and build a unified national forest DBH and carbon sink database to form a comprehensive DBH

monitoring system. In the long term, develop a fully automated unmanned forest survey system suitable for complex stands and terrains, integrate big data and artificial intelligence to achieve real-time dynamic prediction and early warning of forest carbon sinks, and support intelligent forest monitoring. Looking ahead, as sensor costs decrease, intelligent algorithms continue to iterate, and multi-source fusion technologies mature, DBH measurement will overcome current industry pain points and transition from traditional manual surveys to large-scale, long-term, repeatable intelligent monitoring. This will provide efficient and accurate support for national forest resource inventories and dynamic carbon sink monitoring, becoming a practical tool for serving carbon neutrality and promoting sustainable forest management, thereby contributing to global forest ecological protection and sustainable development.

**Author Contributions:** Conceptualization, W.X.; literature review and data collection, G.Z. and Z.L.; writing—original draft preparation, G.Z. and Z.L.; writing—review and editing, G.Z. and Z.L.; supervision and project administration, W.X. All authors have read and agreed to the published version of the manuscript.

**Funding:** This research was funded by the Subproject of the National Key Research and Development Program of China (Grant No. 2025YFC260900204), the Young Scientists Fund of the National Natural Science Foundation of China (Grant No. 42404046), the Project of Guangdong Basic and Applied Basic Research Foundation (Grant No. 2024A1515010447), and the Basic and Applied Basic Research Project under the Basic Research Program of Guangzhou Science and Technology Plan (Grant No. 2023A04J0908).

**Data Availability Statement:** The original contributions presented in the study are included in the article, further inquiries can be directed to the corresponding author.

**Conflicts of Interest:** The authors declare no conflicts of interest.

## References

1. Zhang, J.; Wang, C.; Wang, J.; Huang, X.; Zhou, Z.; Zhou, Z.; Cheng, F. Study on Forest Growing Stock Volume in Kunming City Considering the Relationship Between Stand Density and Allometry. *Forests* **2025**, *16*, 891. [CrossRef]
2. Elzinga, C.; Shearer, R.C.; Elzinga, G. Observer Variation in Tree Diameter Measurements. *West. J. Appl. For.* **2005**, *20*, 134–137. [CrossRef] [PubMed]
3. Johnson, J.E.; Haag, C.L. Reliability of height and diameter remeasurements on Red Pine (*Pinus resinosa* ait.) seedlings. *Agric. Food Sci.* **1985**, *36*, 27–29.
4. McRoberts, R.E.; Hahn, J.T.; Hefty, G.J.; Van, J.R. Variation in forest inventory field measurements. *Can. J. For. Res.* **1994**, *24*, 1766–1770. [CrossRef]
5. Omule, S.A. Personal Bias in Forest Measurements. *For. Chron.* **1980**, *56*, 222–224. [CrossRef]
6. Luoma, V.; Saarinen, N.; Wulder, M.A.; White, J.C.; Vastaranta, M.; Holopainen, M.; Hyyppä, J. Assessing Precision in Conventional Field Measurements of Individual Tree Attributes. *Forests* **2017**, *8*, 38. [CrossRef]
7. Behre, E.C. Comparison of Diameter Tape and Caliper Measurements in Second-Growth Spruce. *J. For.* **1926**, *24*, 178–182. [CrossRef]
8. McArdle, R.E. Relative Accuracy of Calipers and Diameter Tape in Measuring Douglas Fir Trees. *J. For.* **1928**, *26*, 338–342. [CrossRef]
9. Parker, R.C. Nondestructive Sampling Applications of the Tele-Relaskop in Forest Inventory. *S. J. Appl. For.* **1997**, *21*, 75–83. [CrossRef]
10. Feng, Z.K.; Jing, H.T.; Zhou, K.L.; Wu, H.H. Principle and precision evaluation of stem volume surveying by total station. *J. Beijing For. Univ.* **2003**, *25*, 60–63. [CrossRef]
11. Feng, Z.K.; Han, X.C.; Zhou, K.L.; Nan, Y.T.; Fu, X. The analysis of Forestry mensuration principle and precision in fixed samples by total station. *Beijing Surv. Mapp.* **2003**, 28–30. [CrossRef]
12. Hou, X.X.; Tan, Y.S.; Qian, H.; Cheng, P.Y. DBH measurement method based on tree images taken by single-CCD camera mounted on theodolite. *Appl. Res. Comput.* **2014**, *31*, 1225–1228.
13. Parker, R.C.; Matney, T.G. Comparison of Optical Dendrometers for Prediction of Standing Tree Volume. *S. J. Appl. For.* **1999**, *23*, 100–107. [CrossRef]

14. Yan, Q.F. Development of Forestry Digital Measurer of Diameter. *J. Cent. South Univ. For. Technol.* **2008**, *28*, 95–99. [CrossRef]
15. Xu, W.H.; Feng, Z.K.; Su, Z.F.; Xu, H.; Jiao, Y.Q.; Fan, J.C. Development and experiment of handheld digitalized and multi-functional forest measurement gun. *Trans. Chin. Soc. Agric. Eng.* **2013**, *29*, 90–99.
16. Huang, X.D.; Feng, Z.K.; Xie, M.X.; Chen, J.X.; Liu, J.C. Developing and accuracy analysis of portable device for automatically measuring diameter at breast height and tree height. *Trans. Chin. Soc. Agric. Eng.* **2015**, *31*, 92–99.
17. Iglhaut, J.; Cabo, C.; Puliti, S.; Piermattei, L.; O'Connor, J.; Rosette, J. Structure from Motion Photogrammetry in Forestry: A Review. *Curr. For. Rep.* **2019**, *5*, 155–168. [CrossRef]
18. Smith, M.W.; Carrivick, J.L.; Quincey, D.J. Structure from motion photogrammetry in physical geography. *Prog. Phys. Geogr. Earth Environ.* **2015**, *40*, 247–275. [CrossRef]
19. Eltner, A.; Kaiser, A.M.; Fernandez-del Castillo, C.; Rock, G.; Neugirg, F.; Abellán, A. Image-based surface reconstruction in geomorphometry – merits, limits and developments. *Earth Surf. Dyn.* **2016**, *4*, 359–389. [CrossRef]
20. Clark, N.; Wynne, R.H.; Schmoldt, D.L.; Winn, M.F. An assessment of the utility of a non-metric digital camera for measuring standing trees. *Comput. Electron. Agric.* **2000**, *28*, 151–169. [CrossRef]
21. Gaffrey, D.; Fabrika, M.; Smelko, S. Terrestrial single-photogrammetry for measuring standing trees, as applied in the Dobroc virgin forest. *J. For. Sci.* **2001**, *47*, 75–87.
22. Bauwens, S.; Fayolle, A.; Gourlet-Fleury, S.; Ndjele, L.M.; Mengal, C.; Lejeune, P. Terrestrial photogrammetry: A non-destructive method for modelling irregularly shaped tropical tree trunks. *Methods Ecol. Evol.* **2016**, *8*, 460–471. [CrossRef]
23. Surový, P.; Yoshimoto, A.; Panagiotidis, D. Accuracy of Reconstruction of the Tree Stem Surface Using Terrestrial Close-Range Photogrammetry. *Remote Sens.* **2016**, *8*, 123. [CrossRef]
24. Mokroš, M.; Výbošťok, J.; Tomaštík, J.; Grznárová, A.; Valent, P.; Slavík, M.; Merganič, J. High Precision Individual Tree Diameter and Perimeter Estimation from Close-Range Photogrammetry. *Forests* **2018**, *9*, 696. [CrossRef]
25. Mokroš, M.; Liang, X.L.; Surový, P.; Valent, P.; Čerňava, J.; Chudý, F.; Tunák, D.; Saloň, Š.; Merganič, J. Evaluation of Close-Range Photogrammetry Image Collection Methods for Estimating Tree Diameters. *ISPRS Int. J. Geo-Inf.* **2018**, *7*, 93. [CrossRef]
26. Vastaranta, M.; González Latorre, E.; Luoma, V.; Saarinen, N.; Holopainen, M.; Hyyppä, J. Evaluation of a Smartphone App for Forest Sample Plot Measurements. *Forests* **2015**, *6*, 1179–1194. [CrossRef]
27. Gao, Q.; Kan, J. Automatic Forest DBH Measurement Based on Structure from Motion Photogrammetry. *Remote Sens.* **2022**, *14*, 2064. [CrossRef]
28. Liu, J.C.; Feng, Z.K.; Yang, L.Y.; Mannan, A.; Khan, T.U.; Zhao, Z.Y.; Cheng, Z.X. Extraction of Sample Plot Parameters from 3D Point Cloud Reconstruction Based on Combined RTK and CCD Continuous Photography. *Remote Sens.* **2018**, *10*, 1299. [CrossRef]
29. Wu, X.; Zhou, S.; Xu, A.; Chen, B. Passive measurement method of tree diameter at breast height using a smartphone. *Comput. Electron. Agric.* **2019**, *163*, 104875. [CrossRef]
30. Fan, Y.; Feng, Z.; Mannan, A.; Khan, T.; Shen, C.; Saeed, S. Estimating Tree Position, Diameter at Breast Height, and Tree Height in Real-Time Using a Mobile Phone with RGB-D SLAM. *Remote Sens.* **2018**, *10*, 1845. [CrossRef]
31. Song, C.; Yang, B.; Zhang, L.; Wu, D. A handheld device for measuring the diameter at breast height of individual trees using laser ranging and deep-learning based image recognition. *Plant Methods* **2021**, *17*, 67. [CrossRef] [PubMed]
32. Su, J.; Fan, Y.; Mannan, A.; Wang, S.; Long, L.; Feng, Z. Real-Time Estimation of Tree Position, Tree Height, and Tree Diameter at Breast Height Point, Using Smartphones Based on Monocular SLAM. *Forests* **2024**, *15*, 939. [CrossRef]
33. Yang, S.; Xing, Y.; Yin, B.; Wang, D.; Chang, X.; Wang, J. A Novel Method for Extracting DBH and Crown Base Height in Forests Using Small Motion Clips. *Forests* **2024**, *15*, 1635. [CrossRef]
34. Itakura, K.; Hosoi, F. Estimation of tree structure parameters from video frames with removal of blurred images using machine learning. *J. Agric. Meteorol.* **2018**, *74*, 154–161. [CrossRef]
35. Yan, X.H.; Chai, G.Q.; Han, X.Y.; Lei, L.T.; Wang, G.; Jia, X.; Zhang, X.L. SA-Pmnet: Utilizing Close-Range Photogrammetry Combined with Image Enhancement and Self-Attention Mechanisms for 3D Reconstruction of Forests. *Remote Sens.* **2024**, *16*, 416. [CrossRef]
36. Morgenroth, J.; Gomez, C. Assessment of tree structure using a 3D image analysis technique—A proof of concept. *Urban For. Urban Green.* **2014**, *13*, 198–203. [CrossRef]
37. Miller, J.; Morgenroth, J.; Gomez, C. 3D modelling of individual trees using a handheld camera: Accuracy of height, diameter and volume estimates. *Urban For. Urban Green.* **2015**, *14*, 932–940. [CrossRef]
38. Panagiotidis, D.; Surový, P.; Kuželka, K. Accuracy of Structure from Motion models in comparison with terrestrial laser scanner for the analysis of DBH and height influence on error behaviour. *J. For. Sci.* **2016**, *62*, 357–365. [CrossRef]
39. Liang, X.L.; Jaakkola, A.; Wang, Y.S.; Hyyppä, J.; Honkavaara, E.; Liu, J.B.; Kaartinen, H. The Use of a Hand-Held Camera for Individual Tree 3D Mapping in Forest Sample Plots. *Remote Sens.* **2014**, *6*, 6587–6603. [CrossRef]
40. Goodbody, T.R.H.; Coops, N.C.; White, J.C. Digital Aerial Photogrammetry for Updating Area-Based Forest Inventories: A Review of Opportunities, Challenges, and Future Directions. *Curr. For. Rep.* **2019**, *5*, 55–75. [CrossRef]

41. Hemery, G.E.; Savill, P.S.; Pryor, S.N. Applications of the crown diameter–stem diameter relationship for different species of broadleaved trees. *For. Ecol. Manag.* **2005**, *215*, 285–294. [CrossRef]
42. Dandois, J.P.; Ellis, E.C. Remote Sensing of Vegetation Structure Using Computer Vision. *Remote Sens.* **2010**, *2*, 1157–1176. [CrossRef]
43. Ota, T.; Ogawa, M.; Shimizu, K.; Kajisa, T.; Mizoue, N.; Yoshida, S.; Takao, G.; Hirata, Y.; Furuya, N.; Sano, T.; et al. Aboveground Biomass Estimation Using Structure from Motion Approach with Aerial Photographs in a Seasonal Tropical Forest. *Forests* **2015**, *6*, 3882–3898. [CrossRef]
44. Järnstedt, J.; Pekkarinen, A.; Tuominen, S.; Ginzler, C.; Holopainen, M.; Viitala, R. Forest variable estimation using a high-resolution digital surface model. *ISPRS J. Photogramm. Remote Sens.* **2012**, *74*, 78–84. [CrossRef]
45. Wallace, L.; Lucieer, A.; Malenovský, Z.; Turner, D.; Vopěnka, P. Assessment of Forest Structure Using Two UAV Techniques: A Comparison of Airborne Laser Scanning and Structure from Motion (SfM) Point Clouds. *Forests* **2016**, *7*, 62. [CrossRef]
46. Iizuka, K.; Yonehara, T.; Itoh, M.; Kosugi, Y. Estimating Tree Height and Diameter at Breast Height (DBH) from Digital Surface Models and Orthophotos Obtained with an Unmanned Aerial System for a Japanese Cypress (Chamaecyparis obtusa) Forest. *Remote Sens.* **2017**, *10*, 13. [CrossRef]
47. Fritz, A.; Kattenborn, T.; Koch, B. UAV-based photogrammetric point clouds—Tree stem mapping in open stands in comparison to terrestrial laser scanner point clouds. *Int. Arch. Photogramm. Remote Sens. Spat. Inf. Sci.* **2013**, *40*, 141–146. [CrossRef]
48. Cao, L.; Liu, H.; Fu, X.; Zhang, Z.; Shen, X.; Ruan, H. Comparison of UAV LiDAR and Digital Aerial Photogrammetry Point Clouds for Estimating Forest Structural Attributes in Subtropical Planted Forests. *Forests* **2019**, *10*, 145. [CrossRef]
49. Bennett, G.; Hardy, A.; Bunting, P.; Morgan, P.; Fricker, A. A Transferable and Effective Method for Monitoring Continuous Cover Forestry at the Individual Tree Level Using UAVs. *Remote Sens.* **2020**, *12*, 2115. [CrossRef]
50. Almeida, A.; Gonçalves, F.; Silva, G.; Souza, R.; Treuhaft, R.; Santos, W.; Loureiro, D.; Fernandes, M. Estimating Structure and Biomass of a Secondary Atlantic Forest in Brazil Using Fourier Transforms of Vertical Profiles Derived from UAV Photogrammetry Point Clouds. *Remote Sens.* **2020**, *12*, 3560. [CrossRef]
51. Giannetti, F.; Puletti, N.; Puliti, S.; Travaglini, D.; Chirici, G. Assessment of UAV photogrammetric DTM-independent variables for modelling and mapping forest structural indices in mixed temperate forests. *Ecol. Indic.* **2020**, *117*, 106513. [CrossRef]
52. Tinkham, W.T.; Swayze, N.C.; Hoffman, C.M.; Lad, L.E.; Battaglia, M.A. Modeling the Missing DBHs: Influence of Model Form on UAV DBH Characterization. *Forests* **2022**, *13*, 2077. [CrossRef]
53. Kwon, K.; Im, S.; Kim, S.Y.; Lee, Y.; Kwon, C.G. Estimation of Tree Diameter at Breast Height from Aerial Photographs Using a Mask R-CNN and Bayesian Regression. *Forests* **2024**, *15*, 1881. [CrossRef]
54. Xu, J.; Su, M.B.; Sun, Y.X.; Pan, W.B.; Cui, H.C.; Jin, S.; Zhang, L.; Wang, P. Tree Crown Segmentation and Diameter at Breast Height Prediction Based on BlendMask in Unmanned Aerial Vehicle Imagery. *Remote Sens.* **2024**, *16*, 368. [CrossRef]
55. White, J.; Wulder, M.; Vastaranta, M.; Coops, N.; Pitt, D.; Woods, M. The Utility of Image-Based Point Clouds for Forest Inventory: A Comparison with Airborne Laser Scanning. *Forests* **2013**, *4*, 518–536. [CrossRef]
56. Baltsavias, E.P. A comparison between photogrammetry and laser scanning. *ISPRS J. Photogramm. Remote Sens.* **1999**, *54*, 83–94. [CrossRef]
57. Swayze, N.C.; Tinkham, W.T.; Vogeler, J.C.; Hudak, A.T. Influence of flight parameters on UAS-based monitoring of tree height, diameter, and density. *Remote Sens. Environ.* **2021**, *263*, 112540. [CrossRef]
58. Erfanifard, Y.; Hosingholizade, A.; Griess, V.C.; Millan, V.E.G.; Pirasteh, S. Estimating tree diameter at breast height (DBH) from UAV data: A comparison of oblique–Vertical imagery fusion and allometric modeling. *Sci. Remote Sens.* **2025**, *12*, 100331. [CrossRef]
59. Liang, X.L.; Kankare, V.; Hyyppä, J.; Wang, Y.S.; Kukko, A.; Haggrén, H.; Yu, X.W.; Kaartinen, H.; Jaakkola, A.; Guan, F.Y.; et al. Terrestrial laser scanning in forest inventories. *ISPRS J. Photogramm. Remote Sens.* **2016**, *115*, 63–77. [CrossRef]
60. Newnham, G.J.; Armston, J.D.; Calders, K.; Disney, M.I.; Lovell, J.L.; Schaaf, C.B.; Strahler, A.H.; Danson, F.M. Terrestrial Laser Scanning for Plot-Scale Forest Measurement. *Curr. For. Rep.* **2015**, *1*, 239–251. [CrossRef]
61. Calders, K.; Adams, J.; Armston, J.; Bartholomeus, H.; Bauwens, S.; Bentley, L.P.; Chave, J.; Danson, F.M.; Demol, M.; Disney, M.; et al. Terrestrial laser scanning in forest ecology: Expanding the horizon. *Remote Sens. Environ.* **2020**, *251*, 112102. [CrossRef]
62. Li, D.; Yue, C.R. The Application of LiDAR in Inversion of the Forest Parameters. *Geomat. Spat. Inf. Technol.* **2011**, *34*, 54–58.
63. Li, Z.Y.; Liu, Q.W.; Pang, Y. Review on forest parameters inversion using LiDAR. *Natl. Remote Sens. Bull.* **2016**, *20*, 1138–1150. [CrossRef]
64. Simonse, M.; Aschoff, T.; Spiecker, H.; Thies, M. Automatic determination of forest inventory parameters using terrestrial laser scanning. In Proceedings of the Scandinavian Laser Scientific Workshop on Airborne Laser Scanning of Forests, Umea, Sweden, 3–4 September 2003; pp. 251–257.
65. Aschoff, T.; Thies, M.; Spiecker, H. Describing forest stands using terrestrial laser scanning. *Int. Arch. Photogramm. Remote Sens. Spat. Inf. Sci.* **2004**, *35*, 237–241.

66. Bienert, A.; Scheller, S.; Keane, E.; Mohan, F.; Nugent, C. Tree detection and diameter estimations by analysis of forest terrestrial laserscanner point clouds. In *ISPRS Workshop on Laser Scanning*; Citeseer: Hannover, Germany, 2007; Volume 36, pp. 50–55.
67. Maas, H.G.; Bienert, A.; Scheller, S.; Keane, E. Automatic forest inventory parameter determination from terrestrial laser scanner data. *Int. J. Remote Sens.* **2008**, *29*, 1579–1593. [CrossRef]
68. Hopkinson, C.; Chasmer, L.; Young-Pow, C.; Treitz, P. Assessing forest metrics with a ground-based scanning lidar. *Can. J. For. Res.* **2004**, *34*, 573–583. [CrossRef]
69. Watt, P.J.; Donoghue, D.N.M. Measuring forest structure with terrestrial laser scanning. *Int. J. Remote Sens.* **2005**, *26*, 1437–1446. [CrossRef]
70. Liang, X.; Litkey, P.; Hyyppa, J.; Kaartinen, H.; Vastaranta, M.; Holopainen, M. Automatic Stem Mapping Using Single-Scan Terrestrial Laser Scanning. *IEEE Trans. Geosci. Remote Sens.* **2012**, *50*, 661–670. [CrossRef]
71. Ni, W.J.; Guo, Z.F.; Sun, G.Q.; Huang, H.B. Research on extraction of tree structure parameters from terrestrial laser scanner data. *High. Technol. Lett.* **2010**, *20*, 191–198.
72. Liu, C.; Xing, Y.; Duanmu, J.; Tian, X. Evaluating Different Methods for Estimating Diameter at Breast Height from Terrestrial Laser Scanning. *Remote Sens.* **2018**, *10*, 513. [CrossRef]
73. Verhelst, T.E.; Calders, K.; Burt, A.; Demol, M.; D'hont, B.; Nightingale, J.; Terryn, L.; Verbeeck, H. Implications of Pulse Frequency in Terrestrial Laser Scanning on Forest Point Cloud Quality and Individual Tree Structural Metrics. *Remote Sens.* **2024**, *16*, 4560. [CrossRef]
74. Wilkes, P.; Disney, M.; Armston, J.; Bartholomeus, H.; Bentley, L.; Brede, B.; Burt, A.; Calders, K.; Chavana-Bryant, C.; Clewley, D.; et al. TLS2trees: A scalable tree segmentation pipeline for TLS data. *Methods Ecol. Evol.* **2023**, *14*, 3083–3099. [CrossRef]
75. Ma, Z.; Dong, Y.; Zi, J.; Xu, F.; Chen, F. Forest-PointNet: A Deep Learning Model for Vertical Structure Segmentation in Complex Forest Scenes. *Remote Sens.* **2023**, *15*, 4793. [CrossRef]
76. Henrich, J.; van Delden, J.; Seidel, D.; Kneib, T.; Ecker, A.S. TreeLearn: A deep learning method for segmenting individual trees from ground-based LiDAR forest point clouds. *Ecol. Inform.* **2024**, *84*, 102888. [CrossRef]
77. Kulicki, M.; Cabo, C.; Trzciński, T.; Bedkowski, J.; Stereńczak, K. Artificial Intelligence and Terrestrial Point Clouds for Forest Monitoring. *Curr. For. Rep.* **2024**, *11*, 5. [CrossRef]
78. Liu, L.; Pang, Y.; Li, Z.; Xu, G.; Li, D.; Zheng, G. Retrieving structural parameters of individual tree through terrestrial laser scanning data. *J. Remote Sens.* **2014**, *18*, 365–377. [CrossRef]
79. Wang, L.; Lin, W.; Zhang, C.; Ma, J.; Chou, Z.; Li, C. DBH Extraction of Single Wood based on Optimal Slice Thickness Layering Theory and 3D Laser Point Cloud Data. *Remote Sens. Technol. Appl.* **2025**, *40*, 593–599.
80. Zhang, W.; Chen, Y.; Wang, H.; Chen, M.; Wang, X.; Yan, G. Efficient registration of terrestrial LiDAR scans using a coarse-to-fine strategy for forestry applications. *Agric. For. Meteorol.* **2016**, *225*, 8–23. [CrossRef]
81. Guan, H.C.; Su, Y.J.; Sun, X.L.; Xu, G.C.; Li, W.K.; Ma, Q.; Wu, X.Y.; Wu, J.; Liu, L.L.; Guo, Q.H. A marker-free method for registering multi-scan terrestrial laser scanning data in forest environments. *ISPRS J. Photogramm. Remote Sens.* **2020**, *166*, 82–94. [CrossRef]
82. Salvi, J.; Matabosch, C.; Fofi, D.; Forest, J. A review of recent range image registration methods with accuracy evaluation. *Image Vis. Comput.* **2007**, *25*, 578–596. [CrossRef]
83. Tam, G.K.L.; Cheng, Z.Q.; Lai, Y.K.; Langbein, F.C.; Liu, Y.H.; Marshall, D.; Martin, R.R.; Sun, X.F.; Rosin, P.L. Registration of 3D Point Clouds and Meshes: A Survey from Rigid to Nonrigid. *IEEE Trans. Vis. Comput. Graph.* **2013**, *19*, 1199–1217. [CrossRef] [PubMed]
84. Olofsson, K.; Holmgren, J.; Olsson, H. Tree Stem and Height Measurements using Terrestrial Laser Scanning and the RANSAC Algorithm. *Remote Sens.* **2014**, *6*, 4323–4344. [CrossRef]
85. Moskal, L.M.; Zheng, G. Retrieving Forest Inventory Variables with Terrestrial Laser Scanning (TLS) in Urban Heterogeneous Forest. *Remote Sens.* **2011**, *4*, 1–20. [CrossRef]
86. Ritter, T.; Schwarz, M.; Tockner, A.; Leisch, F.; Nothdurft, A. Automatic Mapping of Forest Stands Based on Three-Dimensional Point Clouds Derived from Terrestrial Laser-Scanning. *Forests* **2017**, *8*, 265. [CrossRef]
87. Srinivasan, S.; Popescu, S.; Eriksson, M.; Sheridan, R.; Ku, N.W. Terrestrial Laser Scanning as an Effective Tool to Retrieve Tree Level Height, Crown Width, and Stem Diameter. *Remote Sens.* **2015**, *7*, 1877–1896. [CrossRef]
88. Liu, G.; Wang, J.; Dong, P.; Chen, Y.; Liu, Z. Estimating Individual Tree Height and Diameter at Breast Height (DBH) from Terrestrial Laser Scanning (TLS) Data at Plot Level. *Forests* **2018**, *9*, 398. [CrossRef]
89. Lee, Y.; Lee, J. Evaluation of Accuracy in Estimating Diameter at Breast Height Based on the Scanning Conditions of Terrestrial Laser Scanning and Circular Fitting Algorithm. *Forests* **2024**, *15*, 313. [CrossRef]
90. Li, D.; Pang, Y.; Yue, C.R.; Zhao, D.; Xu, G.C. Extraction of individual tree DBH and height based on terrestrial laser scanner data. *J. Beijing For. Univ.* **2012**, *34*, 79–86. [CrossRef]
91. Bu, G.C.; Wang, P. Adaptive Estimation Method for Diameter at Breast Height Based on Terrestrial Laser Scanning. *Laser Optoelectron. Prog.* **2016**, *53*, 284–292. [CrossRef]

92. Zheng, Y.W.; Wu, J.Z.; Lin, W.S.; Li, X. Extracting Single-tree Structure Parameters of Betula platyphylla by Terrestrial Three-dimensional Laser Scanning. *J. Northeast For. Univ.* **2018**, *46*, 49–55. [CrossRef]
93. Balenović, I.; Liang, X.; Jurjević, L.; Hyyppä, J.; Seletković, A.; Kukko, A. Hand-Held Personal Laser Scanning. *Croat. J. For. Eng.* **2020**, *42*, 165–183. [CrossRef]
94. Wu, Y.; Zhong, S.; Ma, Y.; Zhang, Y.; Liu, M. Application of SLAM-Based Mobile Laser Scanning in Forest Inventory: Methods, Progress, Challenges, and Perspectives. *Forests* **2025**, *16*, 920. [CrossRef]
95. Huang, B.; Zhao, J.; Liu, J. A Survey of Simultaneous Localization and Mapping. *arXiv* **2019**, arXiv:1909.05214.
96. Durrant-Whyte, H.; Bailey, T. Simultaneous localization and mapping: Part I. *IEEE Robot. Autom. Mag.* **2006**, *13*, 99–110. [CrossRef]
97. Liu, G.J.; Huang, K.; Lv, X.L.; Sun, Y.H.; Li, H.L.; Lei, X.H.; Yuan, Q.C.; Shu, L. Innovations and Refinements in LiDAR Odometry and Mapping: A Comprehensive Review. *IEEE/CAA J. Autom. Sin.* **2025**, *12*, 1072–1094. [CrossRef]
98. Zhang, Y.; Shi, P.; Li, J. 3D LiDAR SLAM: A survey. *Photogramm. Rec.* **2024**, *39*, 457–517. [CrossRef]
99. Stal, C.; Verbeurgt, J.; De Sloover, L.; De Wulf, A. Assessment of handheld mobile terrestrial laser scanning for estimating tree parameters. *J. For. Res.* **2020**, *32*, 1503–1513. [CrossRef]
100. Holmgren, J.; Tulldahl, M.; Nordlöf, J.; Willén, E.; Olsson, H. Mobile Laser Scanning for Estimating Tree Stem Diameter Using Segmentation and Tree Spine Calibration. *Remote Sens.* **2019**, *11*, 2781. [CrossRef]
101. Kuželka, K.; Surový, P. Noise Analysis for Unbiased Tree Diameter Estimation from Personal Laser Scanning Data. *Remote Sens.* **2024**, *16*, 1261. [CrossRef]
102. Chudá, J.; Výbošťok, J.; Tomaštík, J.; Chudý, F.; Tunák, D.; Skladan, M.; Tuček, J.; Mokroš, M. Prompt Mapping Tree Positions with Handheld Mobile Scanners Based on SLAM Technology. *Land* **2024**, *13*, 93. [CrossRef]
103. Vatandaşlar, C.; Seki, M.; Zeybek, M. Assessing the potential of mobile laser scanning for stand-level forest inventories in near-natural forests. *For. Int. J. For. Res.* **2023**, *96*, 448–464. [CrossRef]
104. Kükenbrink, D.; Marty, M.; Rehush, N.; Abegg, M.; Ginzler, C. Evaluating the potential of handheld mobile laser scanning for an operational inclusion in a national forest inventory—A Swiss case study. *Remote Sens. Environ.* **2025**, *321*, 114685. [CrossRef]
105. Holvoet, J.; Eichhorn, M.P.; Giannetti, F.; Kükenbrink, D.; Liang, X.L.; Mokroš, M.; Novotný, J.; Pitkänen, T.P.; Puliti, S.; Skudnik, M.; et al. Terrestrial and mobile laser scanning for national forest inventories: From theory to implementation. *Remote Sens. Environ.* **2025**, *329*, 114947. [CrossRef]
106. Ryding, J.; Williams, E.; Smith, M.; Eichhorn, M. Assessing Handheld Mobile Laser Scanners for Forest Surveys. *Remote Sens.* **2015**, *7*, 1095–1111. [CrossRef]
107. Gollob, C.; Ritter, T.; Nothdurft, A. Forest Inventory with Long Range and High-Speed Personal Laser Scanning (PLS) and Simultaneous Localization and Mapping (SLAM) Technology. *Remote Sens.* **2020**, *12*, 1509. [CrossRef]
108. Yang, J.M.; Yuan, W.W.; Lu, H.C.; Liu, Y.H.; Wang, Y.K.; Sun, L.T.; Li, S.M.; Li, H.F. Assessing the Performance of Handheld Laser Scanning for Individual Tree Mapping in an Urban Area. *Forests* **2024**, *15*, 575. [CrossRef]
109. Tupinambá-Simões, F.; Pascual, A.; Guerra-Hernández, J.; Ordóñez, C.; de Conto, T.; Bravo, F. Assessing the Performance of a Handheld Laser Scanning System for Individual Tree Mapping—A Mixed Forests Showcase in Spain. *Remote Sens.* **2023**, *15*, 1169. [CrossRef]
110. Del Perugia, B.; Giannetti, F.; Chirici, G.; Travaglini, D. Influence of Scan Density on the Estimation of Single-Tree Attributes by Hand-Held Mobile Laser Scanning. *Forests* **2019**, *10*, 277. [CrossRef]
111. Bauwens, S.; Bartholomeus, H.; Calders, K.; Lejeune, P. Forest Inventory with Terrestrial LiDAR: A Comparison of Static and Hand-Held Mobile Laser Scanning. *Forests* **2016**, *7*, 127. [CrossRef]
112. Zhou, S.; Kang, F.; Li, W.; Kan, J.; Zheng, Y.; He, G. Extracting Diameter at Breast Height with a Handheld Mobile LiDAR System in an Outdoor Environment. *Sensors* **2019**, *19*, 3212. [CrossRef] [PubMed]
113. Proudman, A.; Ramezani, M.; Digumarti, S.T.; Chebrolu, N.; Fallon, M. Towards real-time forest inventory using handheld LiDAR. *Robot. Auton. Syst.* **2022**, *157*, 104240. [CrossRef]
114. Liang, X.L.; Kukko, A.; Kaartinen, H.; Hyyppä, J.; Yu, X.W.; Jaakkola, A.; Wang, Y.S. Possibilities of a Personal Laser Scanning System for Forest Mapping and Ecosystem Services. *Sensors* **2014**, *14*, 1228–1248. [CrossRef]
115. Holmgren, J.; Tulldahl, H.M.; Nordlöf, J.; Nyström, M.; Olofsson, K.; Rydell, J.; Willén, E. Estimation of tree position and stem diameter using simultaneous localization and mapping with data from a backpack-mounted laser scanner. *Int. Arch. Photogramm. Remote Sens. Spat. Inf. Sci.* **2017**, *42*, 59–63. [CrossRef]
116. Oveland, I.; Hauglin, M.; Gobakken, T.; Næsset, E.; Maalen-Johansen, I. Automatic Estimation of Tree Position and Stem Diameter Using a Moving Terrestrial Laser Scanner. *Remote Sens.* **2017**, *9*, 350. [CrossRef]
117. Oveland, I.; Hauglin, M.; Giannetti, F.; Schipper Kjørsvik, N.; Gobakken, T. Comparing Three Different Ground Based Laser Scanning Methods for Tree Stem Detection. *Remote Sens.* **2018**, *10*, 538. [CrossRef]
118. Hyyppä, E.; Kukko, A.; Kaijaluoto, R.; White, J.C.; Wulder, M.A.; Pyörälä, J.; Liang, X.L.; Yu, X.W.; Wang, Y.S.; Kaartinen, H.; et al. Accurate derivation of stem curve and volume using backpack mobile laser scanning. *ISPRS J. Photogramm. Remote Sens.* **2020**, *161*, 246–262. [CrossRef]

119. Huang, X.; Jia, W.W.; Wang, Q.; Zheng, Y.J.; Liang, Y.Z. Study on Individual Tree Factor Extraction of Larix Olgensis in Backpack Lidar. *For. Eng.* **2019**, *35*, 14–21. [CrossRef]
120. Cai, S.; Xing, Y.Q.; Duanmu, J.L. Extraction of DBH from Filtering out Low Intensity Point Cloud by Backpack Laser Scanning. *For. Eng.* **2021**, *37*, 12–19. [CrossRef]
121. Thomas, S.M.; Chan, Y.T. A simple approach for the estimation of circular arc center and its radius. *Comput. Vis. Graph. Image Process.* **1989**, *45*, 362–370. [CrossRef]
122. Xie, Y.; Zhang, J.; Chen, X.; Pang, S.; Zeng, H.; Shen, Z. Accuracy assessment and error analysis for diameter at breast height measurement of trees obtained using a novel backpack LiDAR system. *For. Ecosyst.* **2020**, *7*, 33. [CrossRef]
123. Choi, K.; Lee, I.; Hong, J.; Oh, T.; Shin, S. Developing a UAV-based rapid mapping system for emergency response. In Proceedings of the Unmanned Systems Technology XI, Orlando, FL, USA, 13–17 April 2009.
124. Nagai, M.; Chen, T.; Shibasaki, R.; Kumagai, H.; Ahmed, A. UAV-Borne 3-D Mapping System by Multisensor Integration. *IEEE Trans. Geosci. Remote Sens.* **2009**, *47*, 701–708. [CrossRef]
125. Miller, R.; Amidi, O. 3-D Site Mapping with the CMU Autonomous Helicopter 3-D Site Mapping with the CMU Autonomous Helicopter. In Proceedings of the 5th International Conference on Intelligent Autonomous Systems, Sapporo, Japan, 1–4 June 1998.
126. Glennie, C. Rigorous 3D error analysis of kinematic scanning LIDAR systems. *J. Appl. Geod.* **2007**, *1*, 147. [CrossRef]
127. Jaakkola, A.; Hyyppä, J.; Kukko, A.; Yu, X.W.; Kaartinen, H.; Lehtomäki, M.; Lin, Y. A low-cost multi-sensoral mobile mapping system and its feasibility for tree measurements. *Isprs J. Photogramm. Remote Sens.* **2010**, *65*, 514–522. [CrossRef]
128. Wallace, L.; Lucieer, A.; Watson, C.; Turner, D. Development of a UAV-LiDAR System with Application to Forest Inventory. *Remote Sens.* **2012**, *4*, 1519–1543. [CrossRef]
129. Jaakkola, A.; Hyyppä, J.; Yu, X.W.; Kukko, A.; Kaartinen, H.; Liang, X.L.; Hyyppä, H.; Wang, Y.S. Autonomous Collection of Forest Field Reference—The Outlook and a First Step with UAV Laser Scanning. *Remote Sens.* **2017**, *9*, 785. [CrossRef]
130. Vandendaele, B.; Fournier, R.A.; Vepakomma, U.; Pelletier, G.; Lejeune, P.; Martin-Ducup, O. Estimation of Northern Hardwood Forest Inventory Attributes Using UAV Laser Scanning (ULS): Transferability of Laser Scanning Methods and Comparison of Automated Approaches at the Tree- and Stand-Level. *Remote Sens.* **2021**, *13*, 2796. [CrossRef]
131. Hackenberg, J.; Spiecker, H.; Calders, K.; Disney, M.; Raumonen, P. SimpleTree —An Efficient Open Source Tool to Build Tree Models from TLS Clouds. *Forests* **2015**, *6*, 4245–4294. [CrossRef]
132. St-Onge, B.; Audet, F.A.; Bégin, J. Characterizing the Height Structure and Composition of a Boreal Forest Using an Individual Tree Crown Approach Applied to Photogrammetric Point Clouds. *Forests* **2015**, *6*, 3899–3922. [CrossRef]
133. Watt, M.S.; Jayathunga, S.; Hartley, R.J.L.; Pearse, G.D.; Massam, P.D.; Cajes, D.; Steer, B.S.C.; Estarija, H.J.C. Use of a Consumer-Grade UAV Laser Scanner to Identify Trees and Estimate Key Tree Attributes across a Point Density Range. *Forests* **2024**, *15*, 899. [CrossRef]
134. Roussel, J.R.; Auty, D.; Coops, N.C.; Tompalski, P.; Goodbody, T.R.H.; Meador, A.S.; Bourdon, J.F.; de Boissieu, F.; Achim, A. lidR: An R package for analysis of Airborne Laser Scanning (ALS) data. *Remote Sens. Environ.* **2020**, *251*, 112061. [CrossRef]
135. Bouvier, M.; Durrieu, S.; Fournier, R.A.; Renaud, J.P. Generalizing predictive models of forest inventory attributes using an area-based approach with airborne LiDAR data. *Remote Sens. Environ.* **2015**, *156*, 322–334. [CrossRef]
136. Tang, J.J.; Chai, Z.Z.; Zhao, Z.W. Remote Sensing Estimation of Individual Tree Diameter at Breast Height Based on Airborne LiDAR Data and Machine Learning Algorithms. *Guangxi Sci.* **2024**, 1–13. [CrossRef]
137. Belgiu, M.; Drăguţ, L. Random forest in remote sensing: A review of applications and future directions. *ISPRS J. Photogramm. Remote Sens.* **2016**, *114*, 24–31. [CrossRef]
138. Kolić, J.; Pernar, R.; Seletković, A.; Ančić, M. Determining the Accuracy of Structural Parameters Measured from LiDAR Images in Lowland Oak Forests. *Forests* **2025**, *16*, 340. [CrossRef]
139. Bruggisser, M.; Hollaus, M.; Otepka, J.; Pfeifer, N. Influence of ULS acquisition characteristics on tree stem parameter estimation. *ISPRS J. Photogramm. Remote Sens.* **2020**, *168*, 28–40. [CrossRef]
140. Pyörälä, J.; Saarinen, N.; Kankare, V.; Coops, N.C.; Liang, X.L.; Wang, Y.S.; Holopainen, M.; Hyyppä, J.; Vastaranta, M. Variability of wood properties using airborne and terrestrial laser scanning. *Remote Sens. Environ.* **2019**, *235*, 111474. [CrossRef]
141. Chisholm, R.A.; Cui, J.; Lum, S.K.Y.; Chen, B.M. UAV LiDAR for below-canopy forest surveys. *J. Unmanned Veh. Syst.* **2013**, *01*, 61–68. [CrossRef]
142. Hyyppä, E.; Hyyppä, J.; Hakala, T.; Kukko, A.; Wulder, M.A.; White, J.C.; Pyörälä, J.; Yu, X.W.; Wang, Y.S.; Virtanen, J.P.; et al. Under-canopy UAV laser scanning for accurate forest field measurements. *ISPRS J. Photogramm. Remote Sens.* **2020**, *164*, 41–60. [CrossRef]
143. Wang, Y.S.; Kukko, A.; Hyyppä, E.; Hakala, T.; Pyörälä, J.; Lehtomäki, M.; El Issaoui, A.; Yu, X.W.; Kaartinen, H.; Liang, X.L.; et al. Seamless integration of above- and under-canopy unmanned aerial vehicle laser scanning for forest investigation. *For. Ecosyst.* **2021**, *8*, 10. [CrossRef]
144. Xu, W.; Cai, Y.; He, D.; Lin, J.; Zhang, F. FAST-LIO2: Fast Direct LiDAR-Inertial Odometry. *IEEE Trans. Robot.* **2022**, *38*, 2053–2073. [CrossRef]

145. Liang, X.; Yao, H.; Qi, H.; Wang, X. Forest in situ observations through a fully automated under-canopy unmanned aerial vehicle. *Geo-Spat. Inf. Sci.* **2024**, *27*, 983–999. [CrossRef]
146. Balestra, M.; Marselis, S.; Sankey, T.T.; Cabo, C.; Liang, X.; Mokroš, M.; Peng, X.; Singh, A.; Stereńczak, K.; Vega, C.; Vincent, G. LiDAR Data Fusion to Improve Forest Attribute Estimates: A Review. *Curr. For. Rep.* **2024**, *10*, 281–297. [CrossRef]
147. Ghamisi, P.; Rasti, B.; Yokoya, N.; Wang, Q.; Hofle, B.; Bruzzone, L.; Bovolo, F.; Chi, M.; Anders, K.; Gloaguen, R.; Atkinson, P.M. Multisource and Multitemporal Data Fusion in Remote Sensing: A Comprehensive Review of the State of the Art. *IEEE Geosci. Remote Sens. Mag.* **2019**, *7*, 6–39. [CrossRef]
148. Schmitt, M.; Zhu, X.X. Data Fusion and Remote Sensing: An ever-growing relationship. *IEEE Geosci. Remote Sens. Mag.* **2016**, *4*, 6–23. [CrossRef]
149. Zhang, J. Multi-source remote sensing data fusion: Status and trends. *Int. J. Image Data Fusion* **2010**, *1*, 5–24. [CrossRef]
150. Polewski, P.; Yao, W.; Cao, L.; Gao, S. Marker-free coregistration of UAV and backpack LiDAR point clouds in forested areas. *ISPRS J. Photogramm. Remote Sens.* **2019**, *147*, 307–318. [CrossRef]
151. Shimizu, K.; Nishizono, T.; Kitahara, F.; Fukumoto, K.; Saito, H. Integrating terrestrial laser scanning and unmanned aerial vehicle photogrammetry to estimate individual tree attributes in managed coniferous forests in Japan. *Int. J. Appl. Earth Obs. Geoinf.* **2022**, *106*, 102658. [CrossRef]
152. Xu, Z.; Cao, L.; Ruan, H.; Li, W.; Jiang, S. Inversion of subtropical forest stand characteristics by integrating very high resolution imagery acquired from UAV and LiDAR point-cloud. *Plant Ecol.* **2015**, *39*, 697–703. [CrossRef]
153. Liu, Y.; Ji, J.; Zhao, L.J.; Feng, W.; He, Q.; Wang, X. Trunk Detection Method Based on Fusion of Lidar and Camera Data. *Southwest Univ.* **2024**, *46*, 183–196. [CrossRef]
154. Singh, A.; Pavlenko, V.; Mokros, M. Tree parameter estimation with iPhone point cloud data using multiple algorithms. *Int. J. Remote Sens.* **2024**, *45*, 9443–9460. [CrossRef]
155. Xiang, W.; Fei, S.; Zhang, S. Single Shot High-Accuracy Diameter at Breast Height Measurement with Smartphone Embedded Sensors. *Sensors* **2025**, *25*, 5060. [CrossRef] [PubMed]


**Disclaimer/Publisher's Note:** The statements, opinions and data contained in all publications are solely those of the individual author(s) and contributor(s) and not of MDPI and/or the editor(s). MDPI and/or the editor(s) disclaim responsibility for any injury to people or property resulting from any ideas, methods, instructions or products referred to in the content.